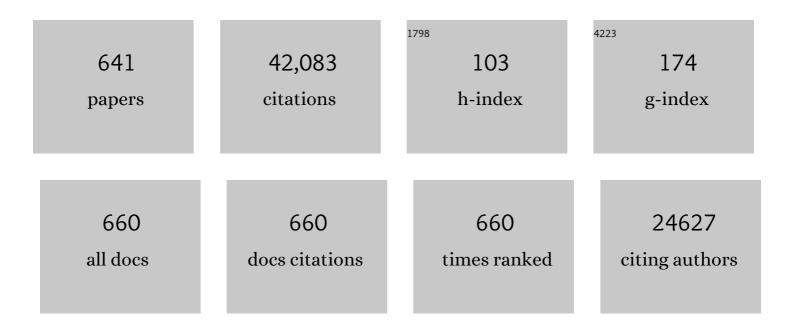
R Jürgen Behm

List of Publications by Year in descending order

Source: https://exaly.com/author-pdf/6015574/publications.pdf Version: 2024-02-01



R IÃ1/ PCEN REHM

#	Article	IF	CITATIONS
1	Oxygen reduction on a high-surface area Pt/Vulcan carbon catalyst: a thin-film rotating ring-disk electrode study. Journal of Electroanalytical Chemistry, 2001, 495, 134-145.	1.9	1,289
2	Scanning tunneling microscopy observations on the reconstructed Au(111) surface: Atomic structure, long-range superstructure, rotational domains, and surface defects. Physical Review B, 1990, 42, 9307-9318.	1.1	1,218
3	Characterization of Highâ€Surfaceâ€Area Electrocatalysts Using a Rotating Disk Electrode Configuration. Journal of the Electrochemical Society, 1998, 145, 2354-2358.	1.3	1,071
4	Novel mechanism for the formation of chemisorption phases: The (2×1)O-Cu(110) â€~ã€~added row'' reconstruction. Physical Review Letters, 1990, 64, 1761-1764.	2.9	497
5	STM investigation of single layer graphite structures produced on Pt(111) by hydrocarbon decomposition. Surface Science, 1992, 264, 261-270.	0.8	494
6	Chemisorption geometry of hydrogen on Ni(111): Order and disorder. Journal of Chemical Physics, 1979, 70, 4168-4184.	1.2	484
7	Kinetics of the Selective CO Oxidation in H2-Rich Gas on Pt/Al2O3. Journal of Catalysis, 1997, 171, 93-105.	3.1	449
8	The Role of Atomic Ensembles in the Reactivity of Bimetallic Electrocatalysts. Science, 2001, 293, 1811-1814.	6.0	439
9	The oxygen reduction reaction on a Pt/carbon fuel cell catalyst in the presence of chloride anions. Journal of Electroanalytical Chemistry, 2001, 508, 41-47.	1.9	425
10	Activation of Molecular Oxygen and the Nature of the Active Oxygen Species for CO Oxidation on Oxide Supported Au Catalysts. Accounts of Chemical Research, 2014, 47, 740-749.	7.6	403
11	Atomic structure of Cu adlayers on Au(100) and Au(111) electrodes observed byin situscanning tunneling microscopy. Physical Review Letters, 1990, 64, 2929-2932.	2.9	396
12	High surface area crystalline titanium dioxide: potential and limits in electrochemical energy storage and catalysis. Chemical Society Reviews, 2012, 41, 5313.	18.7	395
13	Adsorption of hydrogen on Pd(100). Surface Science, 1980, 99, 320-340.	0.8	389
14	Fractal growth of two-dimensional islands: Au on Ru(0001). Physical Review Letters, 1991, 67, 3279-3282.	2.9	375
15	Highly Active and Stable Single-Atom Cu Catalysts Supported by a Metal–Organic Framework. Journal of the American Chemical Society, 2019, 141, 5201-5210.	6.6	361
16	Active Oxygen on a Au/TiO ₂ Catalyst: Formation, Stability, and CO Oxidation Activity. Angewandte Chemie - International Edition, 2011, 50, 10241-10245.	7.2	339
17	Kinetics and Mechanism of the Electrooxidation of Formic Acid—Spectroelectrochemical Studies in a Flow Cell. Angewandte Chemie - International Edition, 2006, 45, 981-985.	7.2	338
18	Interaction of oxygen with Al(111) studied by scanning tunneling microscopy. Journal of Chemical Physics, 1993, 99, 2128-2148.	1.2	326

R Jürgen Behm

#	Article	IF	CITATIONS
19	Adsorption of CO on Pd(100). Journal of Chemical Physics, 1980, 73, 2984-2995.	1.2	316
20	Effect of Temperature on Surface Processes at the Pt(111)â^'Liquid Interface:Â Hydrogen Adsorption, Oxide Formation, and CO Oxidation. Journal of Physical Chemistry B, 1999, 103, 8568-8577.	1.2	315
21	Performance Improvement of Magnesium Sulfur Batteries with Modified Nonâ€Nucleophilic Electrolytes. Advanced Energy Materials, 2015, 5, 1401155.	10.2	308
22	Ethanol Electrooxidation on a Carbon-Supported Pt Catalyst:Â Reaction Kinetics and Product Yields. Journal of Physical Chemistry B, 2004, 108, 19413-19424.	1.2	307
23	Evidence for â€~â€~subsurface'' hydrogen on Pd(110): An intermediate between chemisorbed and dissolve species. Journal of Chemical Physics, 1983, 78, 7486-7490.	² d 1.2	299
24	Surface migration of â€~â€~hot'' adatoms in the course of dissociative chemisorption of oxygen on Al(111 Physical Review Letters, 1992, 68, 624-626.) _{2.9}	297
25	Kinetics of the Selective Low-Temperature Oxidation of CO in H2-Rich Gas over Au∕α-Fe2O3. Journal of Catalysis, 1999, 182, 430-440.	3.1	296
26	Ethanol electro-oxidation on carbon-supported Pt, PtRu and Pt3Sn catalysts: A quantitative DEMS study. Journal of Power Sources, 2006, 154, 351-359.	4.0	296
27	An in-situ scanning tunneling microscopy study of au (111) with atomic scale resolution. Journal of Electroanalytical Chemistry and Interfacial Electrochemistry, 1988, 248, 451-460.	0.3	294
28	Atomic-Resolution Imaging of Close-Packed Metal Surfaces by Scanning Tunneling Microscopy. Physical Review Letters, 1989, 62, 59-62.	2.9	287
29	Surfactant-Induced Layer-by-Layer Growth of Ag on Ag(111): Origins and Side Effects. Physical Review Letters, 1994, 72, 3843-3846.	2.9	284
30	In situ scanning tunnelling microscopy observations of a disorder–order phase transition in hydrogensulfate adlayers on Au(111). Faraday Discussions, 1992, 94, 329-338.	1.6	278
31	Mechanism of the CO-induced1×2→1×1structural transformation of Pt(110). Physical Review Letters, 1989, 63, 1086-1089.	2.9	269
32	Bridge-Bonded Formate:  Active Intermediate or Spectator Species in Formic Acid Oxidation on a Pt Film Electrode?. Langmuir, 2006, 22, 10399-10408.	1.6	264
33	The interaction of CO and Pt(100). I. Mechanism of adsorption and Pt phase transition. Journal of Chemical Physics, 1983, 78, 7437-7447.	1.2	257
34	Performance study of magnesium–sulfur battery using a graphene based sulfur composite cathode electrode and a non-nucleophilic Mg electrolyte. Nanoscale, 2016, 8, 3296-3306.	2.8	247
35	CO adsorption and oxidation on bimetallic Pt/Ru(0001) surfaces – a combined STM and TPD/TPR study. Surface Science, 1998, 411, 249-262.	0.8	236
36	Title is missing!. Catalysis Letters, 2001, 76, 143-150.	1.4	235

#	Article	IF	CITATIONS
37	Toward Highly Reversible Magnesium–Sulfur Batteries with Efficient and Practical Mg[B(hfip) ₄] ₂ Electrolyte. ACS Energy Letters, 2018, 3, 2005-2013.	8.8	234
38	Kinetics, mechanism, and the influence of H2 on the CO oxidation reaction on a Au/TiO2 catalyst. Journal of Catalysis, 2004, 224, 449-462.	3.1	230
39	Electrocatalytic Activity of PtRu Alloy Colloids for CO and CO/H2 Electrooxidation:  Stripping Voltammetry and Rotating Disk Measurements. Langmuir, 1997, 13, 2591-2595.	1.6	227
40	PtRu Alloy Colloids as Precursors for Fuel Cell Catalysts: A Combined XPS, AFM, HRTEM, and RDE Study. Journal of the Electrochemical Society, 1998, 145, 925-931.	1.3	226
41	Strain Relaxation in Hexagonally Close-Packed Metal-Metal Interfaces. Physical Review Letters, 1995, 74, 754-757.	2.9	220
42	Reaction Intermediates and Side Products in the Methanation of CO and CO ₂ over Supported Ru Catalysts in H ₂ -Rich Reformate Gases. Journal of Physical Chemistry C, 2011, 115, 1361-1367.	1.5	219
43	Methanol Oxidation on a Carbon-Supported Pt Fuel Cell CatalystA Kinetic and Mechanistic Study by Differential Electrochemical Mass Spectrometry. Journal of Physical Chemistry B, 2001, 105, 10874-10883.	1.2	218
44	New PtRu Alloy Colloids as Precursors for Fuel Cell Catalysts. Journal of Catalysis, 2000, 195, 383-393.	3.1	217
45	Rotating Disk Electrode Measurements on the CO Tolerance of a High‣urface Area Pt/Vulcan Carbon Fuel Cell Catalyst. Journal of the Electrochemical Society, 1999, 146, 1296-1304.	1.3	214
46	Composition and activity of high surface area PtRu catalysts towards adsorbed CO and methanol electrooxidation—. Electrochimica Acta, 2002, 47, 3693-3706.	2.6	211
47	Impact of the electrolyte salt anion on the solid electrolyte interphase formation in sodium ion batteries. Nano Energy, 2019, 55, 327-340.	8.2	209
48	In-situ STM study of the initial stages of corrosion of Cu(100) electrodes in sulfuric and hydrochloric acid solution. Surface Science, 1998, 399, 49-69.	0.8	201
49	Oxygen Reduction on Ru[sub 1.92]Mo[sub 0.08]SeO[sub 4], Ru/Carbon, and Pt/Carbon in Pure and Methanol-Containing Electrolytes. Journal of the Electrochemical Society, 2000, 147, 2620.	1.3	200
50	Ethanol electrooxidation on novel carbon supported Pt/SnOx/C catalysts with varied Pt:Sn ratio. Electrochimica Acta, 2007, 53, 377-389.	2.6	197
51	Methanol electrooxidation on a colloidal PtRu-alloy fuel-cell catalyst. Electrochemistry Communications, 1999, 1, 1-4.	2.3	196
52	Preferential island nucleation at the elbows of the Au(111) herringbone reconstruction through place exchange. Surface Science, 1996, 365, L647-L651.	0.8	193
53	Kinetics and mechanism of the low-temperature water–gas shift reaction on Au/CeO2 catalysts in an idealized reaction atmosphere. Journal of Catalysis, 2006, 244, 137-152.	3.1	192
54	The interaction of CO and Pt(100). II. Energetic and kinetic parameters. Journal of Chemical Physics, 1983, 78, 7448-7458.	1.2	190

#	Article	IF	CITATIONS
55	Interaction of hydrogen with a palladium (110) surface. Surface Science, 1983, 126, 382-391.	0.8	187
56	Reactive oxygen on a Au/TiO2 supported catalyst. Journal of Catalysis, 2009, 264, 67-76.	3.1	173
57	Adsorption and oxidation of ethanol on colloid-based Pt/C, PtRu/C and Pt3Sn/C catalysts: In situ FTIR spectroscopy and on-line DEMS studies. Physical Chemistry Chemical Physics, 2007, 9, 2686.	1.3	166
58	Activity of PtRuMeOx (Me = W, Mo or V) catalysts towards methanol oxidation and their characterization. Journal of Power Sources, 2002, 105, 297-304.	4.0	162
59	Title is missing!. Catalysis Letters, 2003, 89, 109-114.	1.4	160
60	In-Depth Interfacial Chemistry and Reactivity Focused Investigation of Lithium–Imide- and Lithium–Imidazole-Based Electrolytes. ACS Applied Materials & Interfaces, 2016, 8, 16087-16100.	4.0	159
61	Correlation between CO surface coverage and selectivity/kinetics for the preferential CO oxidation over Pt/γ-Al2O3 and Au/α-Fe2O3: an in-situ DRIFTS study. Journal of Power Sources, 1999, 84, 175-182.	4.0	158
62	Methanol Electrooxidation over Pt/C Fuel Cell Catalysts: Dependence of Product Yields on Catalyst Loading. Langmuir, 2003, 19, 6759-6769.	1.6	158
63	Bimetallic PtSn catalyst for selective CO oxidation in H2-rich gases at low temperatures. Physical Chemistry Chemical Physics, 2001, 3, 1123-1131.	1.3	157
64	Direct observation of surface reactions by scanning tunneling microscopy: Ethylene→ethylidyne→carbon particles→graphite on Pt(111). Journal of Chemical Physics, 1992, 97, 6774-6783.	1.2	155
65	Single step transformation of sulphur to Li2S2/Li2S in Li-S batteries. Scientific Reports, 2015, 5, 12146.	1.6	154
66	Comparative study of imide-based Li salts as electrolyte additives for Li-ion batteries. Journal of Power Sources, 2018, 375, 43-52.	4.0	154
67	Phase transitions of a two-dimensional chemisorbed system: H on Fe(110). Surface Science, 1982, 117, 257-266.	0.8	153
68	Ethanol oxidation on novel, carbon supported Pt alloy catalysts—Model studies under defined diffusion conditions. Electrochimica Acta, 2006, 52, 221-233.	2.6	152
69	Support effects in the Au-catalyzed CO oxidation – Correlation between activity, oxygen storage capacity, and support reducibility. Journal of Catalysis, 2010, 276, 292-305.	3.1	148
70	Ethanol, Acetaldehyde and Acetic Acid Adsorption/Electrooxidation on a Pt Thin Film Electrode under Continuous Electrolyte Flow: An in Situ ATR-FTIRS Flow Cell Study. Journal of Physical Chemistry C, 2010, 114, 9850-9864.	1.5	145
71	Step-flow mechanism versus pit corrosion: scanning-tunneling microscopy observations on wet etching of Si(111) by HF solutions. Chemical Physics Letters, 1991, 186, 275-280.	1.2	142
72	Application of In-situ Attenuated Total Reflection-Fourier Transform Infrared Spectroscopy for the Understanding of Complex Reaction Mechanism and Kinetics: Formic Acid Oxidation on a Pt Film Electrode at Elevated Temperatures. Journal of Physical Chemistry B, 2006, 110, 9534-9544.	1.2	141

#	Article	IF	CITATIONS
73	An in-situ scanning tunneling microscopy study of electrochemically induced "hex―↔ (1 × 1) transitions on Au(100) electrodes. Surface Science, 1993, 296, 310-332.	0.8	138
74	Transport effects in the oxygen reduction reaction on nanostructured, planar glassy carbon supported Pt/GC model electrodes. Physical Chemistry Chemical Physics, 2008, 10, 1931.	1.3	136
75	Correlation between domain boundaries and surface steps: A scanning-tunneling-microscopy study on reconstructed Pt(100). Physical Review Letters, 1986, 56, 228-231.	2.9	129
76	CO ₂ Hydrogenation to Methanol on Supported Au Catalysts under Moderate Reaction Conditions: Support and Particle Size Effects. ChemSusChem, 2015, 8, 456-465.	3.6	127
77	Activation of a Au/CeO2 catalyst for the CO oxidation reaction by surface oxygen removal/oxygen vacancy formation. Journal of Catalysis, 2007, 251, 437-442.	3.1	125
78	Pectin, Hemicellulose, or Lignin? Impact of the Biowaste Source on the Performance of Hard Carbons for Sodiumâ€ion Batteries. ChemSusChem, 2017, 10, 2668-2676.	3.6	125
79	Dendrite Growth in Mg Metal Cells Containing Mg(TFSI) ₂ /Glyme Electrolytes. Journal of the Electrochemical Society, 2018, 165, A1983-A1990.	1.3	124
80	Growth morphology and properties of metals on graphene. Progress in Surface Science, 2015, 90, 397-443.	3.8	123
81	Influence of TiO ₂ Bulk Defects on CO Adsorption and CO Oxidation on Au/TiO ₂ : Electronic Metal–Support Interactions (EMSIs) in Supported Au Catalysts. ACS Catalysis, 2017, 7, 2339-2345.	5.5	120
82	Direct observation of a nucleation and growth process on an atomic scale. Surface Science, 1987, 181, 403-411.	0.8	118
83	Mesoscopic mass transport effects in electrocatalytic processes. Faraday Discussions, 2008, 140, 167-184.	1.6	118
84	The structure of CO adsorbed on Pd(100): A leed and hreels analysis. Surface Science, 1979, 88, L59-L66.	0.8	115
85	Adsorption geometry of hydrogen on Fe(110). Journal of Chemical Physics, 1985, 83, 1959-1968.	1.2	115
86	Homoepitaxial growth on Ni(100) and its modification by a preadsorbed oxygen adlayer. Surface Science, 1993, 284, 154-166.	0.8	114
87	Deactivation of a Au/CeO2 catalyst during the low-temperature water–gas shift reaction and its reactivation: A combined TEM, XRD, XPS, DRIFTS, and activity study. Journal of Catalysis, 2007, 250, 139-150.	3.1	114
88	Fast kinetics of multivalent intercalation chemistry enabled by solvated magnesium-ions into self-established metallic layered materials. Nature Communications, 2018, 9, 5115.	5.8	114
89	STM observations of the initial stages of copper deposition on gold single-crystal electrodes. Journal of Electroanalytical Chemistry and Interfacial Electrochemistry, 1991, 313, 109-119.	0.3	113
90	Selective CO Methanation on Ru/TiO ₂ Catalysts: Role and Influence of Metal–Support Interactions. ACS Catalysis, 2015, 5, 6753-6763.	5.5	113

#	Article	IF	CITATIONS
91	Ethanol electrooxidation on a carbon-supported Pt catalyst at elevated temperature and pressure: A high-temperature/high-pressure DEMS study. Journal of Power Sources, 2009, 190, 2-13.	4.0	112
92	Insights into the reversibility of aluminum graphite batteries. Journal of Materials Chemistry A, 2017, 5, 9682-9690.	5.2	112
93	CuF ₂ as Reversible Cathode for Fluoride Ion Batteries. Advanced Functional Materials, 2017, 27, 1701051.	7.8	112
94	A scanning tunneling microscopy investigation of the structure of the Pt(110) and Au(110) surfaces. Surface Science, 1991, 257, 297-306.	0.8	109
95	Influence of CO2 and H2 on the low-temperature water–gas shift reaction on Au/CeO2 catalysts in idealized and realistic reformate. Journal of Catalysis, 2007, 246, 74-90.	3.1	109
96	The structure of atomic nitrogen adsorbed on Fe(100). Surface Science, 1982, 123, 129-140.	0.8	108
97	Nanomosaic Surfaces by Lateral Phase Separation of a Diblock Copolymer. Macromolecules, 1997, 30, 3874-3880.	2.2	108
98	Superior Lithium Storage Capacity of αâ€MnS Nanoparticles Embedded in Sâ€Doped Carbonaceous Mesoporous Frameworks. Advanced Energy Materials, 2019, 9, 1902077.	10.2	108
99	Summary Abstract: Decomposition of NO on Ag(111) at low temperatures. Journal of Vacuum Science and Technology A: Vacuum, Surfaces and Films, 1984, 2, 1040-1041.	0.9	107
100	Interface structure and misfit dislocations in thin Cu films on Ru(0001). Physical Review B, 1991, 44, 1442-1445.	1.1	107
101	Activity, stability, and deactivation behavior of supported Au/TiO2 catalysts in the CO oxidation and preferential CO oxidation reaction at elevated temperatures. Journal of Catalysis, 2009, 267, 78-88.	3.1	107
102	In situ ATR-FTIRS coupled with on-line DEMS under controlled mass transport conditions—A novel tool for electrocatalytic reaction studies. Electrochimica Acta, 2007, 52, 5634-5643.	2.6	106
103	Adlayer geometry and structural effects in the CO/Ni(110) system. Surface Science, 1985, 160, 387-399.	0.8	105
104	Structure determination of an adsorbate-induced multilayer reconstruction: (1×2)-H/Ni(110). Physical Review Letters, 1987, 58, 148-151.	2.9	105
105	An in-situ STM study of potential-induced changes in the surface topography of Au(100) electrodes. Journal of Electroanalytical Chemistry and Interfacial Electrochemistry, 1990, 290, 21-31.	0.3	105
106	On the CO tolerance of novel colloidal PdAu/carbon electrocatalysts. Journal of Electroanalytical Chemistry, 2001, 501, 132-140.	1.9	105
107	STM imaging and local order of oxygen adlayers on Ni(100). Surface Science, 1991, 245, 255-262.	0.8	104
108	Activity, selectivity, and adsorbed reaction intermediates/reaction side products in the selective methanation of CO in reformate gases on supported Ru catalysts. Journal of Catalysis, 2010, 269, 255-268.	3.1	104

#	Article	IF	CITATIONS
109	Kinetic Isotope Effects in Complex Reaction Networks: Formic Acid Electro-Oxidation. ChemPhysChem, 2007, 8, 380-385.	1.0	103
110	ZnO/ZnFe2O4/N-doped C micro-polyhedrons with hierarchical hollow structure as high-performance anodes for lithium-ion batteries. Nano Energy, 2017, 42, 341-352.	8.2	103
111	CO Oxidation on a Au/TiO ₂ Nanoparticle Catalyst via the Au-Assisted Mars–van Krevelen Mechanism. ACS Catalysis, 2018, 8, 6513-6525.	5.5	103
112	Reconstruction and subsurface lattice distortions in the (2 × 1)O-Ni(110) structure: A LEED analysis. Surface Science, 1990, 225, 171-183.	0.8	100
113	Nucleation and growth of thin metal films on clean and modified metal substrates studied by scanning tunneling microscopy. Journal of Vacuum Science and Technology A: Vacuum, Surfaces and Films, 1992, 10, 1970-1980.	0.9	100
114	Toward the Microscopic Identification of Anions and Cations at the Ionic Liquid Ag(111) Interface: A Combined Experimental and Theoretical Investigation. ACS Nano, 2013, 7, 7773-7784.	7.3	100
115	Development of new anode composite materials for fluoride ion batteries. Journal of Materials Chemistry A, 2014, 2, 20861-20872.	5.2	100
116	Manganese phosphate coated Li[Ni0.6Co0.2Mn0.2]O2 cathode material: Towards superior cycling stability at elevated temperature and high voltage. Journal of Power Sources, 2018, 402, 263-271.	4.0	99
117	Electrooxidation of CO and H2/CO mixtures on a carbon-supported Pt catalystââ,¬â€a kinetic and mechanistic study by differential electrochemical mass spectrometry. Physical Chemistry Chemical Physics, 2001, 3, 4650-4660.	1.3	98
118	A Porphyrin Complex as a Selfâ€Conditioned Electrode Material for Highâ€Performance Energy Storage. Angewandte Chemie - International Edition, 2017, 56, 10341-10346.	7.2	94
119	LEED structure analysis of the clean and (2×1)H covered Pd(110) surface. Journal of Chemical Physics, 1987, 87, 6191-6198.	1.2	93
120	Anisotropy in Nucleation and Growth of Two-Dimensional Islands during Homoepitaxy on "Hex" Reconstructed Au(100). Physical Review Letters, 1994, 73, 553-556.	2.9	91
121	Formic Acid Oxidation on Pure and Bi-Modified Pt(111):Â Temperature Effects. Langmuir, 2000, 16, 8159-8166.	1.6	91
122	CO removal from realistic methanol reformate via preferential oxidation—performance of a Rh/MgO catalyst and comparison to Ru/γ-Al2O3, and Pt/γ-Al2O3. Applied Catalysis B: Environmental, 2004, 50, 209-218.	10.8	90
123	Atomic motion and mass transport in the oxygen induced reconstructions of Cu(110). Journal of Vacuum Science & Technology an Official Journal of the American Vacuum Society B, Microelectronics Processing and Phenomena, 1991, 9, 902.	1.6	88
124	Initial stages of native oxide growth on hydrogen passivated Si(111) surfaces studied by scanning tunneling microscopy. Applied Physics Letters, 1992, 60, 1307-1309.	1.5	88
125	TAP reactor studies of the oxidizing capability of CO2 on a Au/CeO2 catalyst – A first step toward identifying a redox mechanism in the Reverse Water–Gas Shift reaction. Journal of Catalysis, 2013, 302, 20-30.	3.1	88
126	In situ scanning tunneling microscopy observations of the potential-dependent (1 × 2) reconstruction on Au(110) in acidic electrolytes. Surface Science, 1993, 289, 139-151.	0.8	87

#	Article	IF	CITATIONS
127	MnPO ₄ â€Coated Li(Ni _{0.4} Co _{0.2} Mn _{0.4})O ₂ for Lithium(â€Ion) Batteries with Outstanding Cycling Stability and Enhanced Lithiation Kinetics. Advanced Energy Materials, 2018, 8, 1801573.	10.2	87
128	Importance of the additional step-edge barrier in determining film morphology during epitaxial growth. Physical Review B, 1995, 51, 14790-14793.	1.1	86
129	Methanol formation by CO2 hydrogenation on Au/ZnO catalysts – Effect of total pressure and influence of CO on the reaction characteristics. Journal of Catalysis, 2016, 333, 238-250.	3.1	86
130	Electrooxidation of glycerol studied by combined in situ IR spectroscopy and online mass spectrometry under continuous flow conditions. Journal of Electroanalytical Chemistry, 2011, 661, 250-264.	1.9	84
131	Encapsulation of Ru nanoparticles: Modifying the reactivity toward CO and CO2 methanation on highly active Ru/TiO2 catalysts. Applied Catalysis B: Environmental, 2020, 270, 118846.	10.8	84
132	A leed analysis of the (2×1)H-Ni(110) structure. Surface Science, 1987, 186, 45-54.	0.8	82
133	At the ionic liquid metal interface: structure formation and temperature dependent behavior of an ionic liquid adlayer on Au(111). Physical Chemistry Chemical Physics, 2013, 15, 17295.	1.3	82
134	Corrosion of Alkanethiol-Covered Cu(100) Surfaces in Hydrochloric Acid Solution Studied by in-Situ Scanning Tunneling Microscopy. Langmuir, 1997, 13, 7045-7051.	1.6	81
135	VOCl as a Cathode for Rechargeable Chloride Ion Batteries. Angewandte Chemie - International Edition, 2016, 55, 4285-4290.	7.2	81
136	Morphologyâ€Engineered Highly Active and Stable Ru/TiO ₂ Catalysts for Selective CO Methanation. Angewandte Chemie - International Edition, 2019, 58, 10732-10736.	7.2	81
137	Structure and mechanism of alkali-metal-induced reconstruction of fcc (110) surfaces. Physical Review B, 1987, 36, 9267-9270.	1.1	80
138	Interaction of oxygen with Al(111) at elevated temperatures. Journal of Chemical Physics, 1998, 108, 1740-1747.	1.2	80
139	A STM investigation of the nucleation and growth of thin Cu and Au films on Ru(0001). Surface Science, 1991, 251-252, 592-596.	0.8	79
140	Kinetic study of selective CO oxidation in H2-rich gas on a Ru/γ-Al2O3 catalyst. Physical Chemistry Chemical Physics, 2002, 4, 389-397.	1.3	79
141	Surface Formates as Side Products in the Selective CO Oxidation on Pt/\hat{I}^3 -Al2O3. Journal of Catalysis, 1997, 172, 256-258.	3.1	78
142	Formic Acid Electrooxidation on Nobleâ€Metal Electrodes: Role and Mechanistic Implications of pH, Surface Structure, and Anion Adsorption. ChemElectroChem, 2014, 1, 1075-1083.	1.7	77
143	The role of electronic metal-support interactions and its temperature dependence: CO adsorption and CO oxidation on Au/TiO2 catalysts in the presence of TiO2 bulk defects. Journal of Catalysis, 2017, 354, 46-60.	3.1	77
144	Effect of Layer-Dependent Adatom Mobilities in Heteroepitaxial Metal Film Growth: Ni/Ru(0001). Physical Review Letters, 1995, 74, 3864-3867.	2.9	76

#	Article	IF	CITATIONS
145	CO2 reduction on Pt electrocatalysts and its impact on H2 oxidation in CO2 containing fuel cell feed gas – A combined in situ infrared spectroscopy, mass spectrometry and fuel cell performance study. Electrochimica Acta, 2005, 50, 5189-5199.	2.6	76
146	Concentration and Coverage Dependent Adlayer Structures: From Two-Dimensional Networks to Rotation in a Bearing. Journal of Physical Chemistry C, 2010, 114, 1268-1277.	1.5	76
147	Model study on the stability of carbon support materials under polymer electrolyte fuel cell cathode operation conditions. Journal of Power Sources, 2009, 190, 14-24.	4.0	75
148	Selenium and selenium-sulfur cathode materials for high-energy rechargeable magnesium batteries. Journal of Power Sources, 2016, 323, 213-219.	4.0	75
149	Mechanism of an adsorbate-induced surface phase transformation: CO on Pt(100). Surface Science, 1982, 121, L553-L560.	0.8	74
150	Effect of trace amounts of Clâ^' in Cu underpotential deposition on Au(111) in perchlorate solutions: an in-situ scanning tunneling microscopy study. Surface Science, 1995, 335, 129-144.	0.8	74
151	Benzotriazole Adsorption and Inhibition of Cu(100) Corrosion in HCl:  A Combined in Situ STM and in Situ FTIR Spectroscopy Study. Journal of Physical Chemistry B, 1998, 102, 5859-5865.	1.2	74
152	In Situ X-ray Scattering Study of the Passive Film on Ni(111) in Sulfuric Acid Solution. Journal of Physical Chemistry B, 2000, 104, 1222-1226.	1.2	74
153	Inâ€Situ Coating of Li[Ni _{0.33} Mn _{0.33} Co _{0.33}]O ₂ Particles to Enable Aqueous Electrode Processing. ChemSusChem, 2016, 9, 1112-1117.	3.6	74
154	Active Au Species During the Low-Temperature Water Gas Shift Reaction on Au/CeO ₂ : A Time-Resolved Operando XAS and DRIFTS Study. ACS Catalysis, 2017, 7, 6471-6484.	5.5	74
155	Adsorbate-induced step faceting of Cu(100) electrodes in HCl. Surface Science, 1996, 367, L33-L41.	0.8	73
156	The underlayer influence on photoemission and thermal desorption of xenon adsorbed on Ag(111). Journal of Chemical Physics, 1986, 85, 1061-1073.	1.2	72
157	In Situ STM Study of (100) Cu Electrodes in Sulfuric Acid Solution in the Presence of Benzotriazole: Adsorption, Cu Corrosion, and Cu Deposition. Journal of the Electrochemical Society, 1997, 144, L113-L116.	1.3	72
158	PtxRu1â^'x/Ru(0001) surface alloys—formation and atom distribution. Physical Chemistry Chemical Physics, 2008, 10, 3812.	1.3	72
159	Selective CO Methanation on Highly Active Ru/TiO ₂ Catalysts: Identifying the Physical Origin of the Observed Activation/Deactivation and Loss in Selectivity. ACS Catalysis, 2018, 8, 5399-5414.	5.5	72
160	Hydrogen adsorption and coadsorption with CO on well-defined bimetallic PtRu surfaces––a model study on the CO tolerance of bimetallic PtRu anode catalysts in low temperature polymer electrolyte fuel cells. Surface Science, 2003, 541, 137-146.	0.8	71
161	Small Addition of Boron in Palladium Catalyst, Big Improvement in Fuel Cell's Performance: What May Interfacial Spectroelectrochemistry Tell?. ACS Applied Materials & Interfaces, 2016, 8, 7133-7138.	4.0	71
162	Au/TiO ₂ Photo(electro)catalysis: The Role of the Au Cocatalyst in Photoelectrochemical Water Splitting and Photocatalytic H ₂ Evolution. Journal of Physical Chemistry C, 2015, 119, 24750-24759.	1.5	70

#	Article	IF	CITATIONS
163	Further Insights into the Formic Acid Oxidation Mechanism on Platinum: pH and Anion Adsorption Effects. Electrochimica Acta, 2015, 180, 479-485.	2.6	70
164	Complementary Strategies Toward the Aqueous Processing of Highâ€Voltage LiNi _{0.5} Mn _{1.5} O ₄ Lithiumâ€Ion Cathodes. ChemSusChem, 2018, 11, 562-573.	3.6	70
165	A Roadmap for Transforming Research to Invent the Batteries of the Future Designed within the European Large Scale Research Initiative BATTERY 2030+. Advanced Energy Materials, 2022, 12, .	10.2	70
166	Imaging an Ionic Liquid Adlayer by Scanning Tunneling Microscopy at the Solid Vacuum Interface. ChemPhysChem, 2011, 12, 2565-2567.	1.0	69
167	In situSTM study of the electrodeposition and anodic dissolution of ultrathin epitaxial Ni films on Au(111). Physical Review B, 1997, 56, 12506-12518.	1.1	68
168	Sb-enhanced nucleation in the homoepitaxial growth of Ag(111). Physical Review B, 1998, 57, 4127-4131.	1.1	68
169	Interaction of a Self-Assembled Ionic Liquid Layer with Graphite(0001): A Combined Experimental and Theoretical Study. Journal of Physical Chemistry Letters, 2016, 7, 226-233.	2.1	68
170	Wet chemical etching of Si(100) surfaces in concentrated NH4F solution: formation of (2 \tilde{A} — 1)H reconstructed Si(100) terraces versus (111) facetting. Surface Science, 1993, 296, L8-L14.	0.8	67
171	Island-size distributions in submonolayer epitaxial growth: Influence of the mobility of small clusters. Physical Review B, 1996, 53, 4099-4104.	1.1	67
172	Deactivation of Au/CeO2 catalysts during CO oxidation: Influence of pretreatment and reaction conditions. Journal of Catalysis, 2016, 341, 160-179.	3.1	67
173	Negative Charging of Au Nanoparticles during Methanol Synthesis from CO ₂ /H ₂ on a Au/ZnO Catalyst: Insights from Operando IR and Nearâ€Ambientâ€Pressure XPS and XAS Measurements. Angewandte Chemie - International Edition, 2019, 58, 10325-10329.	7.2	67
174	Mechanism of the K-induced reconstruction of Cu(110). Surface Science, 1991, 247, L229-L234.	0.8	66
175	Correlation between local substrate structure and local chemical properties: CO adsorption on well-defined bimetallic surfaces. Surface Science, 1997, 386, 48-55.	0.8	66
176	Reproducibility of highly active Au/TiO2 catalyst preparation and conditioning. Catalysis Letters, 2005, 101, 215-224.	1.4	66
177	Electrochemical oxidation kinetics and mechanism of ethylene glycol on a carbon supported Pt catalyst: A quantitative DEMS study. Journal of Electroanalytical Chemistry, 2006, 595, 23-36.	1.9	66
178	Raising the CO _{<i>x</i>} Methanation Activity of a Ru/γâ€Al ₂ O ₃ Catalyst by Activated Modification of Metal–Support Interactions. Angewandte Chemie - International Edition, 2020, 59, 22763-22770.	7.2	66
179	Influence of the catalyst loading on the activity and the CO selectivity of supported Ru catalysts in the selective methanation of CO in CO2 containing feed gases. Catalysis Today, 2012, 181, 40-51.	2.2	65
180	An STM investigation of the Cu(110)â ^{°,} c(6 × 2)O system. Surface Science, 1990, 240, 151-162.	0.8	64

R Jürgen Behm

#	Article	IF	CITATIONS
181	Overpotential-Controlled Nucleation of Ni Island Arrays on Reconstructed Au(111) Electrode Surfaces. Physical Review Letters, 1996, 77, 5249-5252.	2.9	64
182	In Situ STM Study of Cu(111) Surface Structure and Corrosion in Pure and Benzotriazole-Containing Sulfuric Acid Solution. Journal of Physical Chemistry B, 1999, 103, 10440-10451.	1.2	64
183	Activity, stability and deactivation behavior of Au/CeO2 catalysts in the water gas shift reaction at increased reaction temperature (300°C). Journal of Power Sources, 2009, 190, 64-75.	4.0	64
184	Vanadium Oxychloride/Magnesium Electrode Systems for Chloride Ion Batteries. ACS Applied Materials & Interfaces, 2014, 6, 22430-22435.	4.0	64
185	How Temperature Affects the Mechanism of CO Oxidation on Au/TiO ₂ : A Combined EPR and TAP Reactor Study of the Reactive Removal of TiO ₂ Surface Lattice Oxygen in Au/TiO ₂ by CO. ACS Catalysis, 2016, 6, 5005-5011.	5.5	64
186	Thermal Stability of Au Nanoparticles in O2and Air on Fully Oxidized TiO2(110) Substrates at Elevated Pressures. An AFM/XPS Study of Au/TiO2Model Systems. Journal of Physical Chemistry B, 2004, 108, 19184-19190.	1.2	63
187	STM investigation of the adsorption and temperature dependent reactions of ethylene on Pt(111). Applied Physics A: Solids and Surfaces, 1991, 53, 414-417.	1.4	62
188	Electrochemical Surface Characterization and O2 Reduction Kinetics of Se Surface-Modified Ru Nanoparticle-Based RuSey/C Catalysts. Langmuir, 2006, 22, 10437-10445.	1.6	62
189	Size‧pecific Chemistry on Bimetallic Surfaces: A Combined Experimental and Theoretical Study. ChemPhysChem, 2007, 8, 2068-2071.	1.0	62
190	Phase transitions and domain-wall structures in the K/Cu(110) system: Scanning-tunneling-microscopy observations and Monte Carlo simulations. Physical Review B, 1991, 44, 13689-13702.	1.1	61
191	Simultaneous oxygen reduction and methanol oxidation on a carbon-supported Pt catalyst and mixed potential formation-revisited. Electrochimica Acta, 2004, 49, 3891-3900.	2.6	61
192	Transport Effects in the Electrooxidation of Methanol Studied on Nanostructured Pt/Glassy Carbon Electrodes. Langmuir, 2010, 26, 3569-3578.	1.6	61
193	Selective CO methanation in CO2-rich H2 atmospheres over a Ru/zeolite catalyst: The influence of catalyst calcination. Journal of Catalysis, 2013, 298, 148-160.	3.1	61
194	Ethylene glycol electrooxidation on carbon supported Pt, PtRu and Pt3Sn catalysts—A comparative DEMS study. Journal of Power Sources, 2006, 155, 33-46.	4.0	60
195	Direct Imaging of Adsorption Sites and Local Electronic Bond Effects on a Metal Surface: C/Al(111). Europhysics Letters, 1990, 13, 123-128.	0.7	59
196	In situ video-STM studies of dynamic processes at electrochemical interfaces. Faraday Discussions, 2002, 121, 43-52.	1.6	59
197	Adsorption and electrooxidation of ethylene glycol and its C2 oxidation products on a carbon-supported Pt catalyst: A quantitative DEMS study. Electrochimica Acta, 2009, 54, 6484-6498.	2.6	59
198	The interaction of CO with PdAg/Pd(111) surface alloys—A case study of ensemble effects on a bimetallic surface. Physical Chemistry Chemical Physics, 2011, 13, 10741.	1.3	59

#	Article	IF	CITATIONS
199	Dynamic surface composition in a Mars-van Krevelen type reaction: CO oxidation on Au/TiO2. Journal of Catalysis, 2018, 357, 263-273.	3.1	59
200	A scanning tunneling microscopy investigation of the 1 � 2 ? 1 � 1 structural transformation of the pt(110) surface. Applied Physics A: Solids and Surfaces, 1989, 49, 403-406.	1.4	58
201	High temperature scanning tunneling microscopy studies on the interaction of O2 with Si(111)-(7 × 7) surfaces. Surface Science, 1994, 314, 34-56.	0.8	58
202	Ethanol and Acetaldehyde Adsorption on a Carbon-Supported Pt Catalyst: A Comparative DEMS Study. Fuel Cells, 2004, 4, 113-125.	1.5	58
203	Hierarchical Interactions and Their Influence upon the Adsorption of Organic Molecules on a Graphene Film. Journal of the American Chemical Society, 2011, 133, 9208-9211.	6.6	58
204	Microscopic Aspects of Thin Metal Film Epitaxial Growth on Metallic Substrates. Zeitschrift Fur Elektrotechnik Und Elektrochemie, 1993, 97, 522-537.	0.9	57
205	Mesoscopic structural transformations of the Au(111) surface induced by alkali metal adsorption. Surface Science, 1994, 302, L319-L324.	0.8	57
206	In situSTM studies of Cu underpotential deposition on Au(100) in the presence of sulfate and chloride anions. Physical Review B, 1995, 51, 2484-2490.	1.1	57
207	Activity, Selectivity, and Methanol Tolerance of Se-Modified Ru/C Cathode Catalysts. Journal of Physical Chemistry C, 2007, 111, 1273-1283.	1.5	57
208	Electrodeposition of a Pt Monolayer Film: Using Kinetic Limitations for Atomic Layer Epitaxy. Journal of the American Chemical Society, 2013, 135, 11716-11719.	6.6	57
209	Heteroepitaxial nucleation of diamond on Si(001) in hot filament chemical vapor deposition. Applied Physics Letters, 1995, 66, 1900-1902.	1.5	56
210	High Selectivity of Supported Ru Catalysts in the Selective CO Methanation—Water Makes the Difference. Journal of the American Chemical Society, 2015, 137, 8672-8675.	6.6	56
211	Mechanistic and energetic aspects of the H-induced (1×2) reconstructed structures on Ni(110) and Pd(110). Surface Science, 1987, 189-190, 177-184.	0.8	55
212	Adsorption, surface restructuring and alloy formation in the system. Surface Science, 1995, 341, 62-91.	0.8	55
213	Precise Control of Polydopamine Film Formation by Electropolymerization. Macromolecular Symposia, 2014, 346, 73-81.	0.4	55
214	Potential-Controlled Step Flow to 3D Step Decoration Transition: Ni Electrodeposition on Ag(111). Physical Review Letters, 1999, 83, 5066-5069.	2.9	54
215	Microscopic Electrode Processes in the Four-Electron Oxygen Reduction on Highly Active Carbon-Based Electrocatalysts. ACS Catalysis, 2018, 8, 8162-8176.	5.5	54
216	Nanostructured platinum-on-carbon model electrocatalysts prepared by colloidal lithography. Journal of Electroanalytical Chemistry, 2004, 568, 371-377.	1.9	53

#	Article	IF	CITATIONS
217	Influence of the catalyst surface area on the activity and stability of Au/CeO2 catalysts for the low-temperature water gas shift reaction. Topics in Catalysis, 2007, 44, 183-198.	1.3	53
218	Insights into the electrochemical processes of rechargeable magnesium–sulfur batteries with a new cathode design. Journal of Materials Chemistry A, 2019, 7, 25490-25502.	5.2	53
219	Controlling the O-Vacancy Formation and Performance of Au/ZnO Catalysts in CO ₂ Reduction to Methanol by the ZnO Particle Size. ACS Catalysis, 2021, 11, 9022-9033.	5.5	53
220	CO adsorption kinetics and adlayer build-up studied by combined ATR-FTIR spectroscopy and on-line DEMS under continuous flow conditions. Electrochimica Acta, 2007, 53, 1279-1289.	2.6	52
221	Electrooxidation of ethanol on Pt-based and Pd-based catalysts in alkaline electrolyte under fuel cell relevant reaction and transport conditions. Journal of Power Sources, 2013, 231, 122-133.	4.0	52
222	Au-step atoms as active sites for CO adsorption on Au and bimetallic Au/Pd(111) surfaces. Applied Physics A: Materials Science and Processing, 1998, 66, S513-S517.	1.1	51
223	What drives the selectivity for CO methanation in the methanation of CO2-rich reformate gases on supported Ru catalysts?. Applied Catalysis A: General, 2011, 391, 325-333.	2.2	51
224	In situ STM imaging of high temperature oxygen etching of Si(111)(7 × 7) surfaces. Chemical Physics Letters, 1992, 192, 271-276.	1.2	50
225	The potential of model studies for the understanding of catalyst poisoning and temperature effects in polymer electrolyte fuel cell reactions. Journal of Power Sources, 2006, 154, 327-342.	4.0	50
226	CuCl adlayer formation and Cl induced surface alloying: An in situ STM study on Cu underpotential deposition on Au(110) electrode surfaces. Electrochimica Acta, 1995, 40, 1259-1265.	2.6	48
227	Place-exchange as a mechanism for adlayer island nucleation during epitaxial growth and resulting scaling behavior. Surface Science, 1995, 322, L275-L280.	0.8	48
228	Catalytic Influence of Pt Monolayer Islands on the Hydrogen Electrochemistry of Ru(0001) Studied by Ultrahigh Vacuum Scanning Tunneling Microscopy and Cyclic Voltammetryâ€. Journal of Physical Chemistry B, 2004, 108, 14780-14788.	1.2	48
229	Activity, selectivity, and methanol tolerance of novel carbon-supported Pt and Pt3Me (MeÂ=ÂNi, Co) cathode catalysts. Journal of Applied Electrochemistry, 2007, 37, 1413-1427.	1.5	48
230	Interaction of ionic liquids with noble metal surfaces: structure formation and stability of [OMIM][TFSA] and [EMIM][TFSA] on Au(111) and Ag(111). Physical Chemistry Chemical Physics, 2015, 17, 23816-23832.	1.3	48
231	Adsorption and reaction of sub-monolayer films of an ionic liquid on Cu(111). Chemical Communications, 2014, 50, 8601-8604.	2.2	47
232	CO ₂ Reduction to Methanol on Au/CeO ₂ Catalysts: Mechanistic Insights from Activation/Deactivation and SSITKA Measurements. ACS Catalysis, 2020, 10, 3580-3594.	5.5	47
233	Scanning tunneling microscopy studies on the growth and structure of thin metallic films on metal substrates. Journal of Vacuum Science & Technology an Official Journal of the American Vacuum Society B, Microelectronics Processing and Phenomena, 1992, 10, 256.	1.6	46
234	In-situ video-STM studies of Cu electrodeposition on Cu(100) in HCl solution. Electrochimica Acta, 2003, 48, 2915-2921.	2.6	46

#	Article	IF	CITATIONS
235	Selective oxidation of CO on Ru/l ³ -Al2O3 in methanol reformate at low temperatures. Applied Catalysis B: Environmental, 2004, 52, 123-134.	10.8	46
236	Influence of the crystalline phase and surface area of the TiO2 support on the CO oxidation activity of mesoporous Au/TiO2 catalysts. Applied Catalysis B: Environmental, 2009, 91, 470-480.	10.8	46
237	X-ray photoelectron spectrum in surface interfacing of gold nanoparticles with polymer molecules in a hybrid nanocomposite structure. Nanotechnology, 2009, 20, 075701.	1.3	46
238	Ethanol oxidation on shape-controlled platinum nanoparticles at different pHs: A combined in situ IR spectroscopy and online mass spectrometry study. Journal of Electroanalytical Chemistry, 2016, 763, 116-124.	1.9	46
239	Metal–Organic Framework Derived Fe ₇ S ₈ Nanoparticles Embedded in Heteroatomâ€Doped Carbon with Lithium and Sodium Storage Capability. Small Methods, 2020, 4, 2000637.	4.6	46
240	Investigation on the formation of Mg metal anode/electrolyte interfaces in Mg/S batteries with electrolyte additives. Journal of Materials Chemistry A, 2020, 8, 22998-23010.	5.2	46
241	Two-Dimensional Needle Growth of Electrodeposited Ni on Reconstructed Au(111). Physical Review Letters, 1996, 77, 3165-3168.	2.9	45
242	Bi adsorption on Pt(111) in perchloric acid solution: A rotating ring–disk electrode and XPS study. Physical Chemistry Chemical Physics, 2000, 2, 4379-4386.	1.3	45
243	Structure and local reactivity of PdAg/Pd(111) surface alloys. Physical Chemistry Chemical Physics, 2013, 15, 1497-1508.	1.3	45
244	Adsorption of the ionic liquid [BMP][TFSA] on Au(111) and Ag(111): substrate effects on the structure formation investigated by STM. Beilstein Journal of Nanotechnology, 2013, 4, 903-918.	1.5	45
245	Side reactions and stability of pre-treated carbon felt electrodes for vanadium redox flow batteries: A DEMS study. Carbon, 2020, 158, 580-587.	5.4	45
246	Atomic scale characterization of oxygen adsorbates on Al(111) by scanning tunneling microscopy. Applied Physics A: Solids and Surfaces, 1988, 47, 99-102.	1.4	44
247	Determination of nanometer structures and surface roughness of polished Si wafers by scanning tunneling microscopy. Journal of Applied Physics, 1991, 69, 4273-4281.	1.1	44
248	Interaction of CO with PdCu surface alloys supported on Ru(0001). Surface Science, 2004, 558, 181-194.	0.8	44
249	Electrochemical and compositional characterization of solid interphase layers in an interface-modified solid-state Li–sulfur battery. Journal of Materials Chemistry A, 2020, 8, 16451-16462.	5.2	44
250	Electronic metal-support interactions and their promotional effect on CO2 methanation on Ru/ZrO2 catalysts. Journal of Catalysis, 2021, 400, 407-420.	3.1	44
251	Geometry of hydrogen chemisorption on Ni(111) analyzed by low energy electron diffraction. Solid State Communications, 1978, 28, 373-376.	0.9	43
252	Catalytic activity of nanostructured Au: Scale effects versus bimetallic/bifunctional effects in low-temperature CO oxidation on nanoporous Au. Beilstein Journal of Nanotechnology, 2013, 4, 111-128.	1.5	43

#	ARTICLE	IF	CITATIONS
253	Methanol synthesis via CO ₂ hydrogenation over a Au/ZnO catalyst: an isotope labelling study on the role of CO in the reaction process. Physical Chemistry Chemical Physics, 2016, 18, 10781-10791.	1.3	43
254	Electro-Oxidation of Ethylene Glycol on a Pt-Film Electrode Studied by Combined in Situ Infrared Spectroscopy and Online Mass Spectrometry. Journal of Physical Chemistry C, 2012, 116, 2872-2883.	1.5	42
255	A combined UHV-STM-flow cell set-up for electrochemical/electrocatalytic studies of structurally well-defined UHV prepared model electrodes. Physical Chemistry Chemical Physics, 2017, 19, 4166-4178.	1.3	42
256	Insight into Sulfur Confined in Ultramicroporous Carbon. ACS Omega, 2018, 3, 11290-11299.	1.6	42
257	Reducing Capacity and Voltage Decay of Coâ€Free Li _{1.2} Ni _{0.2} Mn _{0.6} O ₂ as Positive Electrode Material for Lithium Batteries Employing an Ionic Liquidâ€Based Electrolyte. Advanced Energy Materials, 2020, 10, 2001830.	10.2	42
258	Electrooxidation of acetaldehyde on carbon-supported Pt, PtRu and Pt3Sn and unsupported PtRu0.2 catalysts: A quantitative DEMS study. Journal of Applied Electrochemistry, 2006, 36, 1187-1198.	1.5	41
259	Hydrogen adsorption on bimetallic PdAu(111) surface alloys: minimum adsorption ensemble, ligand and ensemble effects, and ensemble confinement. Physical Chemistry Chemical Physics, 2014, 16, 23930-23943.	1.3	41
260	Conversion/alloying lithium-ion anodes – enhancing the energy density by transition metal doping. Sustainable Energy and Fuels, 2018, 2, 2601-2608.	2.5	41
261	Influence of CO on the Activation, O-Vacancy Formation, and Performance of Au/ZnO Catalysts in CO ₂ Hydrogenation to Methanol. Journal of Physical Chemistry Letters, 2019, 10, 3645-3653.	2.1	41
262	Reconstructive adsorption of Na on Al(111) studied by scanning tunneling microscopy. Physical Review B, 1995, 51, 13592-13613.	1.1	40
263	Formation of two-dimensional sulfide phases on Al(111): an STM study. Surface Science, 1995, 324, 91-105.	0.8	40
264	Interaction of CO with atomically well-defined Pt Ru /Ru(0 0 0 1) surface alloys. Surface Science, 2007, 601, 4608-4619.	0.8	40
265	Formation, stability and CO adsorption properties of PdAg/Pd(111) surface alloys. Surface Science, 2009, 603, 1046-1054.	0.8	40
266	On the Role of Residual Ag in Nanoporous Au Catalysts for CO Oxidation: A Combined Microreactor and TAP Reactor Study. ChemCatChem, 2012, 4, 251-259.	1.8	40
267	Selective CO methanation on isostructural Ru nanocatalysts: The role of support effects. Journal of Catalysis, 2019, 373, 103-115.	3.1	40
268	Model calculation for the tunnel current from a tungsten tip to a Ni(100) surface with a chemisorbed oxygen atom. Journal of Vacuum Science and Technology A: Vacuum, Surfaces and Films, 1988, 6, 327-330.	0.9	39
269	Scanning-tunneling-microscope imaging of clean and alkali-metal-covered Cu(110) and Au(110) surfaces. Physical Review B, 1993, 48, 1738-1749.	1.1	39
270	Nanoscale Pattern Formation during Electrodeposition: Ru on Reconstructed Au(111). Physical Review Letters, 1999, 83, 3246-3249.	2.9	39

#	Article	IF	CITATIONS
271	A novel dual thin-layer flow cell double-disk electrode design for kinetic studies on supported catalysts under controlled mass-transport conditions. Electrochimica Acta, 2004, 49, 1297-1305.	2.6	39
272	Interaction of CO with planar Au/TiO2 model catalysts at elevated pressures. Topics in Catalysis, 2007, 44, 83-93.	1.3	39
273	Influence of H2, CO2 and H2O on the activity and deactivation behavior of Au/CeO2 catalysts in the water gas shift reaction at 300°C. Applied Catalysis B: Environmental, 2010, 95, 57-70.	10.8	39
274	Reactive removal of surface oxygen by H ₂ , CO and CO/H ₂ on a Au/CeO ₂ catalyst and its relevance to the preferential CO oxidation (PROX) and reverse water gas shift (RWGS) reaction. Catalysis Science and Technology, 2015, 5, 925-941.	2.1	39
275	Development of a water based process for stable conversion cathodes on the basis of FeF3. Journal of Power Sources, 2016, 313, 213-222.	4.0	39
276	Revisiting the Electrochemical Lithiation Mechanism of Aluminum and the Role of Liâ€rich Phases (Li _{1+<i>x</i>} Al) on Capacity Fading. ChemSusChem, 2019, 12, 2609-2619.	3.6	39
277	Unveiling the Intricate Intercalation Mechanism in Manganese Sesquioxide as Positive Electrode in Aqueous Znâ€Metal Battery. Advanced Energy Materials, 2021, 11, 2100962.	10.2	39
278	Initial stages of metal encapsulation during epitaxial growth studied by STM: Rh/Ag(100). Physical Review B, 1996, 53, 13747-13752.	1.1	38
279	Structure and growth of ultrathin titanium oxide films on Ru(0001). Surface Science, 2005, 576, 29-44.	0.8	38
280	Au/TiO2/Ru(0001) model catalysts and their interaction with CO. Surface Science, 2006, 600, 4992-5003.	0.8	38
281	Structure Formation in Bis(terpyridine) Derivative Adlayers:  Moleculeâ^'Substrate versus Moleculeâ^'Molecule Interactions. Langmuir, 2007, 23, 11570-11579.	1.6	38
282	On the origin of the selectivity in the preferential CO oxidation on Au/TiO2 – Nature of the active oxygen species for H2 oxidation. Journal of Catalysis, 2014, 317, 272-276.	3.1	38
283	Oxygen Reduction on Structurally Well Defined, Bimetallic PtRu Surfaces: Monolayer PtxRu1â^'x/Ru(0001) Surface Alloys Versus Pt Film Covered Ru(0001). Topics in Catalysis, 2014, 57, 222-235.	1.3	38
284	Stabilizing shallow color centers in diamond created by nitrogen delta-doping using SF6 plasma treatment. Applied Physics Letters, 2015, 106, .	1.5	38
285	Room Temperature CO _{ad} Desorption/Exchange Kinetics on Pt Electrodes—A Combined In Situ IR and Mass Spectrometry Study. ChemPhysChem, 2007, 8, 2484-2489.	1.0	37
286	Formation, atomic distribution and mixing energy in two-dimensional PdxAg1â^'x surface alloys on Pd(111). Physical Chemistry Chemical Physics, 2012, 14, 10754.	1.3	37
287	Oxidation of the Partly Oxidized Ethylene Glycol Oxidation Products Glycolaldehyde, Glyoxal, Glycolic Acid, Glyoxylic Acid, and Oxalic Acid on Pt Electrodes: A Combined ATR-FTIRS and DEMS Spectroelectrochemical Study. Journal of Physical Chemistry C, 2013, 117, 12689-12701.	1.5	37
288	Borohydride electrooxidation over Pt/C, AuPt/C and Au/C catalysts: Partial reaction pathways and mixed potential formation. Electrochemistry Communications, 2015, 60, 9-12.	2.3	37

#	Article	IF	CITATIONS
289	Highly Reversible Sodiation of Tin in Glyme Electrolytes: The Critical Role of the Solid Electrolyte Interphase and Its Formation Mechanism. ACS Applied Materials & Interfaces, 2020, 12, 3697-3708.	4.0	37
290	On the Kinetics and Mechanism of the Oxygen Induced (2 × 1) Reconstruction of Ni(HO). Zeitschrift Fur Elektrotechnik Und Elektrochemie, 1986, 90, 294-297.	0.9	36
291	Controlling the Interparticle Spacing of Auâ^'Salt Loaded Micelles and Au Nanoparticles on Flat Surfaces. Langmuir, 2007, 23, 10150-10155.	1.6	36
292	Intermolecular vs molecule–substrate interactions: A combined STM and theoretical study of supramolecular phases on graphene/Ru(0001). Beilstein Journal of Nanotechnology, 2011, 2, 365-373.	1.5	36
293	Dynamic studies of CO oxidation on nanoporous Au using a TAP reactor. Journal of Catalysis, 2011, 278, 219-227.	3.1	36
294	Potentialâ€Induced Surface Restructuring—The Need for Structural Characterization in Electrocatalysis Research. Angewandte Chemie - International Edition, 2014, 53, 12936-12940.	7.2	36
295	Nitrogen Rich Hierarchically Organized Porous Carbon/Sulfur Composite Cathode Electrode for High Performance Li/S Battery: A Mechanistic Investigation by Operando Spectroscopic Studies. Advanced Materials Interfaces, 2016, 3, 1600372.	1.9	36
296	Spatially Resolved Chemistry on Bimetallic Surfaces. Acta Physica Polonica A, 1998, 93, 259-272.	0.2	36
297	Scanning tunneling microscopy observation of phase-transition phenomena in the Cs/Cu(110) system: Evidence for a two-step disordering mechanism of a uniaxial (1×3) phase. Physical Review Letters, 1992, 69, 2547-2550.	2.9	35
298	Distance dependence and corrugation in barrier-height measurements on metal surfaces. Ultramicroscopy, 1992, 42-44, 533-540.	0.8	35
299	Interaction of platinum colloids with single crystalline oxide and graphite substrates: a combined AFM, STM and XPS study. Catalysis Letters, 1996, 37, 35-39.	1.4	35
300	Interaction of SiH4 with Si(100)2×1 and with Si(111)7×7 at 690 K: A comparative scanning tunneling microscopy study. Journal of Vacuum Science and Technology A: Vacuum, Surfaces and Films, 1996, 14, 1499-1504.	0.9	35
301	New DRIFTS Cell Design for the Simultaneous Acquisition of IR Spectra and Kinetic Data Using On-Line Product Analysis. Applied Spectroscopy, 2001, 55, 1537-1543.	1.2	35
302	Low-temperature water-gas shift reaction on Au/CeO2 catalysts – the influence of catalyst pre-treatment on the activity and deactivation in idealized reformate. Catalysis Letters, 2007, 116, 105-115.	1.4	35
303	Submicron-sized silicon oxycarbide spheres as anodes for alkali ion batteries. Journal of Materials Chemistry A, 2015, 3, 23707-23715.	5.2	35
304	Interaction of the ionic liquid [BMP][TFSA] with rutile TiO ₂ (110) and coadsorbed lithium. Physical Chemistry Chemical Physics, 2016, 18, 6618-6636.	1.3	35
305	On the formation and bonding of a surface carbonate on Ni(100). Surface Science, 1991, 255, 327-343.	0.8	34
306	Chemical oxidation of hydrogen passivated Si(111) surfaces in H2O2. Journal of Applied Physics, 1995, 78, 4131-4136.	1.1	34

#	Article	IF	CITATIONS
307	Reversible place-exchange during film growth: a mechanism for surfactant transport. Surface Science, 1996, 355, L375-L380.	0.8	34
308	Electrocatalysis and transport effects on nanostructured Pt/GC electrodes. Journal of Electroanalytical Chemistry, 2010, 644, 90-102.	1.9	34
309	Iron encapsulated nitrogen and sulfur co-doped few layer graphene as a non-precious ORR catalyst for PEMFC application. RSC Advances, 2015, 5, 66494-66501.	1.7	34
310	A novel DEMS approach for studying gas evolution at battery-type electrode electrolyte interfaces: High-voltage LiNi0.5Mn1.5O4 cathode in ethylene and dimethyl carbonate electrolytes. Electrochimica Acta, 2019, 314, 188-201.	2.6	34
311	Step Faceting: Origin of the Temperature Dependent Induction Period in Ni(100) Oxidation. Physical Review Letters, 1995, 74, 1399-1402.	2.9	33
312	The structure, growth and reactivity of electrodeposited Ru/Au(111) surfaces. Journal of Electroanalytical Chemistry, 2001, 500, 479-490.	1.9	33
313	The effect of ammonium ions on oxygen reduction and hydrogen peroxide formation on polycrystalline Pt electrodes. Journal of Power Sources, 2008, 176, 435-443.	4.0	33
314	New Insights into the Mechanism and Kinetics of Adsorbed CO Electrooxidation on Platinum: Online Mass Spectrometry and Kinetic Monte Carlo Simulation Studies. Journal of Physical Chemistry C, 2012, 116, 11040-11053.	1.5	33
315	Oxygen Activity in Li-Rich Disordered Rock-Salt Oxide and the Influence of LiNbO ₃ Surface Modification on the Electrochemical Performance. Chemistry of Materials, 2019, 31, 4330-4340.	3.2	33
316	The oxidation of CO on pt(100): Mechanism and structure. Surface Science, 1984, 147, 143-161.	0.8	32
317	Defects on the Pt(100) surface and their influence on surface reactions—A scanning tunneling microscopy study. IBM Journal of Research and Development, 1986, 30, 403-410.	3.2	32
318	Fabrication of Pt/Ru Nanoparticle Pair Arrays with Controlled Separation and their Electrocatalytic Properties. ACS Nano, 2011, 5, 2547-2558.	7.3	32
319	Ex situ testing method to characterize cathode catalysts degradation under simulated start-up/shut-down conditions – A contribution to polymer electrolyte membrane fuel cell benchmarking. Journal of Power Sources, 2012, 215, 266-273.	4.0	32
320	Excellent Cycling Stability and Superior Rate Capability of Na ₃ V ₂ (PO ₄) ₃ Cathodes Enabled by Nitrogenâ€Doped Carbon Interpenetration for Sodiumâ€Ion Batteries. ChemElectroChem, 2017, 4, 1256-1263.	1.7	32
321	Avoiding Selfâ€Poisoning: A Key Feature for the High Activity of Au/Mg(OH) ₂ Catalysts in Continuous Lowâ€Temperature CO Oxidation. Angewandte Chemie - International Edition, 2017, 56, 9597-9602.	7.2	32
322	Computer simulations of the adsorbate-induced structural transformation of Pt(100). Surface Science, 1989, 218, 452-466.	0.8	31
323	In situ STM study of electrodeposition and anodic dissolution of Ni on Ag(111). Physical Chemistry Chemical Physics, 2001, 3, 3351-3363.	1.3	31
324	Diffusion-limited electrodeposition of ultrathin Au films on Pt(111). Surface Science, 2004, 572, 115-125.	0.8	31

#	Article	IF	CITATIONS
325	Maleimido-Terminated Self-Assembled Monolayers. Chemistry - A European Journal, 2005, 11, 3968-3978.	1.7	31
326	Design and characterization of a temporal analysis of products reactor. Review of Scientific Instruments, 2007, 78, 104103.	0.6	31
327	Study of all solid-state rechargeable fluoride ion batteries based on thin-film electrolyte. Journal of Solid State Electrochemistry, 2017, 21, 1243-1251.	1.2	31
328	A Porphyrin Complex as a Self onditioned Electrode Material for Highâ€Performance Energy Storage. Angewandte Chemie, 2017, 129, 10477-10482.	1.6	31
329	Oxygen Reduction and Evolution on Niâ€modified Co ₃ O ₄ (1 1 1) Cathodes for Zn–Air Batteries: A Combined Surface Science and Electrochemical Model Study. ChemSusChem, 2020, 13, 3199-3211.	3.6	31
330	A comparative STM study of the growth of thin Au films on clean and oxygen-precovered Ru(0001) surfaces. Ultramicroscopy, 1992, 42-44, 475-482.	0.8	30
331	Surface alloy formation, short-range order, and deuterium adsorption properties of monolayer PdRu/Ru(0001) surface alloys. Surface Science, 2009, 603, 1439-1455.	0.8	30
332	Interaction of Hydrogen with Bimetallic Surfaces. Zeitschrift Fur Physikalische Chemie, 2009, 223, 9-36.	1.4	30
333	Interaction of CO with Structurally Well-Defined Monolayer PtAu/Pt(111) Surface Alloys. Journal of Physical Chemistry C, 2012, 116, 11154-11165.	1.5	30
334	Reactive Interaction of (Sub-)monolayers and Multilayers of the Ionic Liquid 1-Butyl-1-methylpyrrolidinium Bis(trifluoro-methylsulfonyl)imide with Coadsorbed Lithium on Cu(111). Journal of Physical Chemistry C, 2015, 119, 16649-16659.	1.5	30
335	Oxygen reduction and evolution in an ionic liquid ([BMP][TFSA]) based electrolyte: A model study of the cathode reactions in Mg-air batteries. Journal of Power Sources, 2016, 333, 173-183.	4.0	30
336	Introducing Highly Redoxâ€Active Atomic Centers into Insertionâ€Type Electrodes for Lithiumâ€Ion Batteries. Advanced Energy Materials, 2020, 10, 2000783.	10.2	30
337	Reversible Copper Sulfide Conversion in Nonflammable Trimethyl Phosphate Electrolytes for Safe Sodiumâ€Ion Batteries. Small Structures, 2021, 2, 2100035.	6.9	30
338	Bridging the pressure and material gap in heterogeneous catalysis. Physical Chemistry Chemical Physics, 2007, 9, 3459.	1.3	29
339	From Adlayer Islands to Surface Alloy: Structural and Chemical Changes on Bimetallic PtRu/Ru(0001) Surfaces. ChemPhysChem, 2010, 11, 3123-3132.	1.0	29
340	Pt promotion and spill-over processes during deposition and desorption of upd-Had and OHad on PtxRu1â^'x/Ru(0001) surface alloys. Physical Chemistry Chemical Physics, 2010, 12, 10388.	1.3	29
341	Combining Optimized Particle Morphology with a Niobiumâ€Based Coating for Long Cyclingâ€Life, Highâ€Voltage Lithiumâ€Ion Batteries. ChemSusChem, 2016, 9, 1670-1679.	3.6	29
342	Ultrafast Ionic Liquid-Assisted Microwave Synthesis of SnO Microflowers and Their Superior Sodium-Ion Storage Performance. ACS Applied Materials & Interfaces, 2017, 9, 26797-26804.	4.0	29

#	Article	IF	CITATIONS
343	The system K/Au(111): adsorption and surface restructuring. Surface Science, 1996, 348, 280-286.	0.8	28
344	Increasing the creation yield of shallow single defects in diamond by surface plasma treatment. Applied Physics Letters, 2013, 103, .	1.5	28
345	Oxygen reduction reaction activity and long-term stability of platinum nanoparticles supported on titania and titania-carbon nanotube composites. Journal of Power Sources, 2018, 400, 580-591.	4.0	28
346	Influence of adsorbed oxygen on the tunnel current from an Al(111) surface. Journal of Microscopy, 1988, 152, 687-695.	0.8	27
347	Ordered structures and structural transformations on a K-covered Au(110) surface. Surface Science, 1991, 253, 270-282.	0.8	27
348	Double-layer structure, corrosion and corrosion inhibition of copper in aqueous solution. Applied Physics A: Materials Science and Processing, 1998, 66, S447-S451.	1.1	27
349	Comparative In Situ STM Studies on the Electrodeposition of Ultrathin Nickel Films on Ag(111) and Au(111) Electrodes. Journal of the Electrochemical Society, 1999, 146, 1013-1018.	1.3	27
350	On the Morphology and Stability of Au Nanoparticles on TiO2(110) Prepared from Micelle-Stabilized Precursors. Langmuir, 2006, 22, 7873-7880.	1.6	27
351	On the Role of Reactant Transport and (Surface) Alloy Formation for the CO Tolerance of Carbon Supported PtRu Polymer Electrolyte Fuel Cell Catalysts. Fuel Cells, 2006, 6, 190-202.	1.5	27
352	A new allotropic structure of silver nanocrystals nucleated and grown over planar polymer molecules. Philosophical Magazine Letters, 2007, 87, 361-372.	0.5	27
353	Electrooxidation of ethylene glycol on a carbon-supported Pt catalyst at elevated temperatures and pressure: A high-temperature/high-pressure DEMS study. Journal of Electroanalytical Chemistry, 2010, 644, 103-109.	1.9	27
354	Methanol Oxidation Over a Pt/C Catalyst at High Temperatures and Pressure: An Online Electrochemical Mass Spectrometry Study. Journal of Physical Chemistry C, 2010, 114, 22573-22581.	1.5	27
355	Directed assembly of Ru nanoclusters on Ru(0001)-supported graphene: STM studies and atomistic modeling. Physical Review B, 2012, 86, .	1.1	27
356	The influence of reactive side products on the electrooxidation of methanol – a combined in situ infrared spectroscopy and online mass spectrometry study. Physical Chemistry Chemical Physics, 2014, 16, 13780-13799.	1.3	27
357	Exploring SnS nanoparticles interpenetrated with high concentration nitrogen-doped-carbon as anodes for sodium ion batteries. Electrochimica Acta, 2019, 296, 806-813.	2.6	27
358	Effects of SiO2-doping on high-surface-area Ru/TiO2 catalysts for the selective CO methanation. Applied Catalysis B: Environmental, 2021, 282, 119483.	10.8	27
359	In situ STM imaging of spontaneously deposited ruthenium on Au(). Surface Science, 2002, 517, 207-218.	0.8	26
360	Interaction of Deuterium with Well-Defined Pt _{<i>x</i>} Ru _{1â^'<i>x</i>} /Ru(0001) Surface Alloys. Journal of Physical Chemistry C, 2008, 112, 8381-8390.	1.5	26

#	Article	IF	CITATIONS
361	Entropic stabilization of large adsorbates on weakly binding substrates—a thermal desorption and scanning tunneling microscopy study. Physical Chemistry Chemical Physics, 2010, 12, 818-822.	1.3	26
362	Molecular approaches towards mixed metal oxides and their behaviour in mixed oxide support Au catalysts for CO oxidation. Dalton Transactions, 2011, 40, 3269.	1.6	26
363	Oxidation of 1-propanol on a Pt film electrode studied by combined electrochemical, in situ IR spectroscopy and online mass spectrometry measurements. Electrochimica Acta, 2013, 104, 505-517.	2.6	26
364	Mechanistic aspects of the electro-oxidation of ethylene glycol on a Pt-film electrode: A combined in situ IR spectroscopy and online mass spectrometry study of kinetic isotope effects. Catalysis Today, 2013, 202, 154-162.	2.2	26
365	VOCI as a Cathode for Rechargeable Chloride Ion Batteries. Angewandte Chemie, 2016, 128, 4357-4362.	1.6	26
366	Performance of titanium oxynitrides in the electrocatalytic oxygen evolution reaction. Nano Energy, 2016, 29, 136-148.	8.2	26
367	Island Assisted Surface Alloying Observed after Ni Deposition onAu(110)â^'(1×2). Physical Review Letters, 1996, 76, 2535-2538.	2.9	25
368	LOW ADATOM MOBILITY ON THE (1 \tilde{A} — 2)-MISSING-ROW RECONSTRUCTED Au(110) SURFACE. Surface Review and Letters, 1997, 04, 1103-1108.	0.5	25
369	Simulated "Air Bleed―Oxidation of Adsorbed CO on Carbon Supported Pt. Part 2. Electrochemical Measurements of Hydrogen Peroxide Formation during O2Reduction in a Double-Disk Electrode Dual Thin-Layer Flow Cell. Journal of Physical Chemistry B, 2004, 108, 7893-7901.	1.2	25
370	Stable active oxygen on mesoporous Au/TiO2 supported catalysts and its correlation with the CO oxidation activity. Journal of Catalysis, 2009, 266, 299-307.	3.1	25
371	Novel N, C doped Ti(IV)-oxides as Pt-free catalysts for the O 2 reduction reaction. Electrochimica Acta, 2014, 146, 335-345.	2.6	25
372	Steering the selectivity in CO2 reduction on highly active Ru/TiO2 catalysts: Support particle size effects. Journal of Catalysis, 2021, 401, 160-173.	3.1	25
373	K-induced restructuring of Au(001) observed by scanning tunneling microscopy. Surface Science, 1994, 302, 158-170.	0.8	24
374	Scanning-tunneling-microscopy observation of K-induced reconstructions on Au(110). Physical Review B, 1995, 51, 4402-4414.	1.1	24
375	On the potential-dependent etching of Si(111) in aqueous NH4F solution. Surface Science, 1998, 396, 198-211.	0.8	24
376	Structure and growth in metal epitaxy on low-index Au surfaces—a comparison between solidâ^£electrolyte and solidâ^£vacuum interfaces. Journal of Electroanalytical Chemistry, 1999, 467, 258-269.	1.9	24
377	Structure–reactivity correlation in the oxygen reduction reaction: Activity of structurally well defined Au Pt1â^'/Pt(111) monolayer surface alloys. Journal of Electroanalytical Chemistry, 2014, 716, 71-79.	1.9	24
378	Silicon carboxylate derived silicon oxycarbides as anodes for lithium ion batteries. Journal of Materials Chemistry A, 2017, 5, 10190-10199.	5.2	24

#	Article	IF	CITATIONS
379	Rechargeable Calcium–Sulfur Batteries Enabled by an Efficient Borateâ€Based Electrolyte. Small, 2020, 16, e2001806.	5.2	24
380	Approaching the low-temperature limit in nucleation and two-dimensional growth of fcc (100) metal films Ag/Ag(100). Physical Review B, 2002, 66, .	1.1	23
381	Interaction of Cu atoms with ordered 2D oligopyridine networks. Surface Science, 2007, 601, 4200-4205.	0.8	23
382	Mesoporous Au/TiO2 Catalysts for Low Temperature CO Oxidation. Catalysis Letters, 2007, 119, 199-208.	1.4	23
383	Membrane Fuel Cell Cathode Catalysts Based on Titanium Oxide Supported Platinum Nanoparticles. ChemPhysChem, 2014, 15, 2094-2107.	1.0	23
384	A Novel Approach for Differential Electrochemical Mass Spectrometry Studies on the Decomposition of Ionic Liquids. Electrochimica Acta, 2016, 197, 290-299.	2.6	23
385	Synthesis of amorphous and graphitized porous nitrogen-doped carbon spheres as oxygen reduction reaction catalysts. Beilstein Journal of Nanotechnology, 2020, 11, 1-15.	1.5	23
386	Atomic step resolution in scanning tunneling microscope imaging of H2SO4covered Si(100) surfaces. Applied Physics Letters, 1991, 58, 1027-1029.	1.5	22
387	Potential dependent etching of Si(111) surfaces in NH4F solutions studied by scanning tunneling microscopy. Applied Physics Letters, 1993, 62, 2516-2518.	1.5	22
388	Gas phase etching of Si(111)-(7×7) surfaces by oxygen observed by scanning tunneling microscopy. Journal of Vacuum Science & Technology an Official Journal of the American Vacuum Society B, Microelectronics Processing and Phenomena, 1993, 11, 1955.	1.6	22
389	The kinetics of phase transitions in underpotentially deposited Cu adlayers on Au(111). Physical Chemistry Chemical Physics, 2000, 2, 4387-4392.	1.3	22
390	Formation and short-range order of two-dimensionalCuxPd1â^'xmonolayer surface alloys onRu(0001). Physical Review B, 2006, 73, .	1.1	22
391	Energetics driving the short-range order in CuxPd1–x/Ru(0001) monolayer surface alloys. Physical Chemistry Chemical Physics, 2007, 9, 5127.	1.3	22
392	Potential-Induced COadIsland Formation on a Platinum Thin-Film Electrode in the H-upd Potential Region. Journal of Physical Chemistry C, 2007, 111, 435-438.	1.5	22
393	Interaction of Mass Transport and Reaction Kinetics during Electrocatalytic CO Oxidation in a Thin-Layer Flow Cell. Journal of Physical Chemistry C, 2011, 115, 468-478.	1.5	22
394	Interaction of CO and deuterium with bimetallic, monolayer Pt-island/film covered Ru(0001) surfaces. Physical Chemistry Chemical Physics, 2012, 14, 10919.	1.3	22
395	On the nature of the active Au species: CO oxidation on cyanide leached Au/TiO2 catalysts. Catalysis Today, 2015, 244, 146-160.	2.2	22
396	Interlayerâ€Expanded Vanadium Oxychloride as an Electrode Material for Magnesiumâ€Based Batteries. ChemElectroChem, 2017, 4, 738-745.	1.7	22

#	Article	IF	CITATIONS
397	Intercalation and Deintercalation of Lithium at the Ionic Liquid–Graphite(0001) Interface. Journal of Physical Chemistry Letters, 2017, 8, 5804-5809.	2.1	22
398	The Effect of Anions and pH on the Activity and Selectivity of an Annealed Polycrystalline Au Film Electrode in the Oxygen Reduction Reactionâ€Revisited. ChemPhysChem, 2019, 20, 3276-3288.	1.0	22
399	The role of nitrogen-doping and the effect of the pH on the oxygen reduction reaction on highly active nitrided carbon sphere catalysts. Electrochimica Acta, 2019, 299, 736-748.	2.6	22
400	Zincâ€ion Hybrid Supercapacitors Employing Acetateâ€Based Waterâ€inâ€Salt Electrolytes. Small, 2022, 18, .	5.2	22
401	Summary Abstract: The formation of a surface carbonate species on Ni(100) by reaction between oxygen and CO2. Journal of Vacuum Science and Technology A: Vacuum, Surfaces and Films, 1983, 1, 1223-1224.	0.9	21
402	Atomic structure of clean and Cu covered Pt(110) electrodes. Surface Science, 1995, 336, 19-26.	0.8	21
403	Electrochemical Deposition of Platinum Hydrosol on Graphite Observed by Scanning Tunneling Microscopy. Journal of Catalysis, 1996, 163, 492-495.	3.1	21
404	Fabrication of surface nanostructures by scanning tunneling microscope induced decomposition of SiH[sub 4] and SiH[sub 2]Cl[sub 2]. Journal of Vacuum Science & Technology an Official Journal of the American Vacuum Society B, Microelectronics Processing and Phenomena, 1997, 15, 1373.	1.6	21
405	Nanostructured Pt/GC Model Electrodes Prepared by the Deposition of Metal-Salt-Loaded Micelles. Langmuir, 2007, 23, 5795-5801.	1.6	21
406	Complete Quantitative Online Analysis of Methanol Electrooxidation Products via Electron Impact and Electrospray Ionization Mass Spectrometry. Analytical Chemistry, 2012, 84, 5479-5483.	3.2	21
407	Electrooxidation of acetaldehyde on a carbon supported Pt catalyst at elevated temperature/pressure: An on-line differential electrochemical mass spectrometry study. Journal of Power Sources, 2012, 204, 1-13.	4.0	21
408	Competition of CO and H2 for Active Oxygen Species during the Preferential CO Oxidation (PROX) on Au/TiO2 Catalysts. Catalysts, 2016, 6, 21.	1.6	21
409	Water assisted dispersion of Ru nanoparticles: The impact of water on the activity and selectivity of supported Ru catalysts during the selective methanation of CO in CO2-rich reformate. Journal of Catalysis, 2016, 335, 79-94.	3.1	21
410	Effect of titania surface modification of mesoporous silica SBA-15 supported Au catalysts: Activity and stability in the CO oxidation reaction. Journal of Catalysis, 2017, 356, 214-228.	3.1	21
411	Embedding Heterostructured αâ€MnS/MnO Nanoparticles in Sâ€Doped Carbonaceous Porous Framework as Highâ€Performance Anode for Lithiumâ€ion Batteries. ChemElectroChem, 2021, 8, 918-927.	1.7	21
412	Site selective SiH4 adsorption on Si(111)(7 × 7) surfaces. Surface Science, 1995, 325, L441-L447.	0.8	20
413	Combined work function and STM study on growth, alloying and oxidation of epitaxial aluminum films on Ru(0001). Surface Science, 1996, 345, L11-L18.	0.8	20
414	Local arrangement of silylene groups on Si(100)2×1 afterSiH4sdecomposition. Physical Review B, 1997, 55, 4659-4664.	1.1	20

#	Article	IF	CITATIONS
415	On the origin of Ru bilayer island growth on Pt(111). Vacuum, 2009, 84, 13-18.	1.6	20
416	Short-Range Order in a Metalâ [^] Organic Network. Journal of Physical Chemistry C, 2009, 113, 21265-21268.	1.5	20
417	Electrooxidation of 1-Propanol on Pt — Mechanistic Insights from a Spectro-Electrochemical Study using Isotope Labeling. Journal of Physical Chemistry C, 2012, 116, 25852-25867.	1.5	20
418	Atomic-Scale Processes in Cu Corrosion and Corrosion Inhibition. MRS Bulletin, 1999, 24, 16-23.	1.7	19
419	Initial stages of the anodic etching of aluminum foils studied by atomic force microscopy. Corrosion Science, 1999, 41, 35-55.	3.0	19
420	The role of surface defects in large organic molecule adsorption: substrate configuration effects. Physical Chemistry Chemical Physics, 2012, 14, 10726.	1.3	19
421	Shape-selected nanocrystals for in situ spectro-electrochemistry studies on structurally well defined surfaces under controlled electrolyte transport: A combined in situ ATR-FTIR/online DEMS investigation of CO electrooxidation on Pt. Beilstein Journal of Nanotechnology, 2014, 5, 735-746.	1.5	19
422	Electrochemical stability and restructuring and its impact on the electro-oxidation of CO: Pt modified Ru(0001) electrodes. Surface Science, 2015, 631, 248-257.	0.8	19
423	Synthesis and electrocatalytic performance of spherical core-shell tantalum (oxy)nitride@nitrided carbon composites in the oxygen reduction reaction. Electrochimica Acta, 2017, 227, 367-381.	2.6	19
424	Electro-oxidation of methanol on Ru-core Pt-shell type model electrodes. Electrochimica Acta, 2019, 311, 244-254.	2.6	19
425	Imaging of individual atoms on an Al(111) surface by scanning tunnelling microscopy. Journal of Microscopy, 1988, 152, 423-425.	0.8	18
426	Microstructured Au/TiO2Model Catalyst Systems. Langmuir, 2004, 20, 6644-6650.	1.6	18
427	Scanning mass spectrometer for quantitative reaction studies on catalytically active microstructures. Review of Scientific Instruments, 2007, 78, 084104.	0.6	18
428	Nanostructured, Glassy-Carbon-Supported Pt/GC Electrodes: The Presence of Secondary Pt Nanostructures and How to Avoid Them. Journal of the Electrochemical Society, 2008, 155, K171.	1.3	18
429	CO oxidation on planar Au/TiO2 model catalysts: Deactivation and the influence of water. Vacuum, 2009, 84, 193-196.	1.6	18
430	Quantitative Online Analysis of Liquid-Phase Products of Methanol Oxidation in Aqueous Sulfuric Acid Solutions Using Electrospray Ionization Mass Spectrometry. Analytical Chemistry, 2010, 82, 2472-2479.	3.2	18
431	Differential Electrochemical Mass Spectrometry of Carbon Felt Electrodes for Vanadium Redox Flow Batteries. ACS Applied Energy Materials, 2018, 1, 6714-6718.	2.5	18
432	Superoxide formation in Li ₂ VO ₂ F cathode material – a combined computational and experimental investigation of anionic redox activity. Journal of Materials Chemistry A, 2020, 8, 16551-16559.	5.2	18

R Jürgen Behm

#	Article	IF	CITATIONS
433	Summary Abstract: The hexagonal reconstruction of Pt(100): A scanning tunneling microscopy study. Journal of Vacuum Science and Technology A: Vacuum, Surfaces and Films, 1986, 4, 1330-1331.	0.9	17
434	Reconstruction in a thin film: Epitaxial Pt on Pd(100). Surface Science, 1987, 189-190, 1069-1075.	0.8	17
435	Writing electronically active nanometerâ€scale structures with a scanning tunneling microscope. Applied Physics Letters, 1991, 59, 2136-2138.	1.5	17
436	Simulated â€~air bleed' oxidation of adsorbed CO on carbon supported Pt. Journal of Electroanalytical Chemistry, 2003, 554-555, 427-437.	1.9	17
437	Coverage dependent structures of oligopyridine adlayers on (111) oriented Ag films. Physical Chemistry Chemical Physics, 2007, 9, 5672.	1.3	17
438	Chemical properties of structurally well-defined PdRu/Ru(0001) surface alloys – Interaction with CO. Surface Science, 2009, 603, 1456-1466.	0.8	17
439	Insights into solid electrolyte interphase formation on alternative anode materials in lithium-ion batteries. Journal of Applied Electrochemistry, 2017, 47, 249-259.	1.5	17
440	High activity and negative apparent activation energy in low-temperature CO oxidation – present on Au/Mg(OH) ₂ , absent on Au/TiO ₂ . Catalysis Science and Technology, 2017, 7, 4145-4161.	2.1	17
441	Structure formation and surface chemistry of ionic liquids on model electrode surfaces—Model studies for the electrode electrolyte interface in Li-ion batteries. Journal of Chemical Physics, 2018, 148, 193821.	1.2	17
442	Summary Abstract: Kinetics and mechanism of the oxygen induced surface reconstruction on Ni(110). Journal of Vacuum Science and Technology A: Vacuum, Surfaces and Films, 1985, 3, 1595-1596.	0.9	16
443	Small-volume, ultrahigh-vacuum-compatible high-pressure reaction cell for combined kinetic and in situ IR spectroscopic measurements on planar model catalysts. Review of Scientific Instruments, 2005, 76, 123903.	0.6	16
444	Stability of Nanostructured Pt/Glassy Carbon Electrodes Prepared by Colloidal Lithography. Journal of the Electrochemical Society, 2008, 155, K50.	1.3	16
445	From bilayer to monolayer growth: Temperature effects in the growth of Ru on Pt(111). Surface Science, 2009, 603, 2556-2563.	0.8	16
446	Interaction of C ₁ Molecules with a Pt Electrode at Open Circuit Potential: A Combined Infrared and Mass Spectroscopic Study. Journal of Physical Chemistry C, 2014, 118, 6799-6808.	1.5	16
447	Inhibitor-assisted synthesis of silica-core microbeads with pepsin-imprinted nanoshells. Journal of Materials Chemistry B, 2016, 4, 4462-4469.	2.9	16
448	Understanding the Origin of Higher Capacity for Ni-Based Disordered Rock-Salt Cathodes. Chemistry of Materials, 2020, 32, 3447-3461.	3.2	16
449	Scanning Tunneling Microscopy. Springer Series in Surface Sciences, 1986, , 361-411.	0.3	16
450	Coadsorption of hydrogen and CO on well-defined Pt35Ru65/Ru(0001) surface alloys—site specificity vs. adsorbate–adsorbate interactions. Physical Chemistry Chemical Physics, 2010, 12, 9801.	1.3	15

#	Article	IF	CITATIONS
451	Structure Formation and Thermal Stability of Mono- and Multilayers of Ethylene Carbonate on Cu(111): A Model Study of the Electrode Electrolyte Interface. Journal of Physical Chemistry C, 2016, 120, 16791-16803.	1.5	15
452	Infrared spectroscopy via substrate-integrated hollow waveguides: a powerful tool in catalysis research. Analyst, The, 2016, 141, 5990-5995.	1.7	15
453	A Lithiumâ€lon Battery with Enhanced Safety Prepared using an Environmentally Friendly Process. ChemSusChem, 2016, 9, 1290-1298.	3.6	15
454	Selective Modification and Probing of the Electrocatalytic Activity of Step Sites. Journal of the American Chemical Society, 2020, 142, 1278-1286.	6.6	15
455	Anodic molecular hydrogen formation on Ru and Cu electrodes. Catalysis Science and Technology, 2020, 10, 6870-6878.	2.1	15
456	Performance of Au/ZnO catalysts in CO2 reduction to methanol: Varying the Au loading / Au particle size. Applied Catalysis A: General, 2021, 624, 118318.	2.2	15
457	<i>In situ</i> , atomic scale observation of electrode topography and reactions. Journal of Microscopy, 1988, 152, 537-540.	0.8	14
458	XPS investigation of low-temperature adsorption and thermal desorption of N2O on Ag(111). Journal of Electron Spectroscopy and Related Phenomena, 1990, 52, 175-183.	0.8	14
459	Interactions between alkali metals and oxygen on a reconstructed surface: An STM study of oxygen adsorption on the alkali-metal-covered Cu(110) surface. Physical Review B, 1994, 50, 17456-17462.	1.1	14
460	SiH4 chemical vapor deposition on Si(111)-(7×7) studied by scanning tunneling microscopy. Surface Science, 1997, 385, 123-145.	0.8	14
461	DEMS Analysis of Small Organic Molecule Electrooxidation: A High-Temperature High-Pressure DEMS study. ECS Transactions, 2008, 16, 1243-1251.	0.3	14
462	Segregation and Stability in Surface Alloys: PdxRu1â^'x/Ru(0001) and PtxRu1â^'x/Ru(0001). ChemPhysChem, 2011, 12, 1148-1154.	1.0	14
463	Growth of PtRu Clusters on Ru(0001)‣upported Monolayer Graphene Films. ChemPhysChem, 2012, 13, 3313-3319.	1.0	14
464	Improved Performance of Ru/γâ€Al ₂ O ₃ Catalysts in the Selective Methanation of CO in CO ₂ 2â€Rich Reformate Gases upon Transient Exposure to Waterâ€Containing Reaction Gas. ChemSusChem, 2015, 8, 3869-3881.	3.6	14
465	Electroless deposition of Au/Pt/Pd nanoparticles on p-Si(111) for the light-induced hydrogen evolution reaction. Catalysis Today, 2015, 244, 3-9.	2.2	14
466	Electrochemical Characterization and Stability of Ag _{<i>x</i>} Pt _{1–<i>x</i>} /Pt(111) Surface Alloys. Journal of Physical Chemistry C, 2016, 120, 16179-16190.	1.5	14
467	Performance Improvement of V–Fe–Cr–Ti Solid State Hydrogen Storage Materials in Impure Hydrogen Gas. ACS Applied Materials & Interfaces, 2018, 10, 1662-1671.	4.0	14
468	On the Role of the Support in Pt Anode Catalyst Degradation under Simulated H ₂ Fuel Starvation Conditions. Journal of the Electrochemical Society, 2018, 165, J3342-J3349.	1.3	14

#	Article	IF	CITATIONS
469	Experimental and Computational Study on the Interaction of an Ionic Liquid Monolayer with Lithium on Pristine and Lithiated Graphite. Journal of Physical Chemistry C, 2018, 122, 18968-18981.	1.5	14
470	Model Studies on the Solid Electrolyte Interphase Formation on Graphite Electrodes in Ethylene Carbonate and Dimethyl Carbonate: Highly Oriented Pyrolytic Graphite. ChemElectroChem, 2019, 6, 4985-4997.	1.7	14
471	Rotational epitaxy vs. missing row reconstruction: Au/Cu/Au(110). Surface Science, 1997, 388, L1100-L1106.	0.8	13
472	Admetal-induced substrate surface restructuring during metal-on-metal electrochemical deposition studied by in situ scanning tunneling microscopy. Surface Science, 2000, 460, 249-263.	0.8	13
473	The Influence of Reactive Side Products in Electrocatalytic Reactions: Methanol Oxidation as Case Study. ChemPhysChem, 2013, 14, 3678-3681.	1.0	13
474	Electrochemical Test Procedures for Accelerated Evaluation of Fuel Cell Cathode Catalyst Degradation. Fuel Cells, 2014, 14, 378-385.	1.5	13
475	Perfluoroalkyl-Phosphonic Acid Adsorption on Polycrystalline Platinum and Its Influence on the Oxygen Reduction Reaction. Journal of Physical Chemistry C, 2015, 119, 18859-18869.	1.5	13
476	Spherical Core–Shell Titanium (Oxy)nitride@Nitrided Carbon Composites as Catalysts for the Oxygen Reduction Reaction: Synthesis and Electrocatalytic Performance. ChemElectroChem, 2016, 3, 1641-1654.	1.7	13
477	The Application of Scanning Tunneling Microscopy to Electrochemistry. , 1992, , 275-292.		12
478	Potential-Induced Strain Relaxation in Au Mono- and Bilayer Films on Pt(111) Electrode Surfaces. Physical Review Letters, 2003, 90, 056102.	2.9	12
479	High-pressure study on the adsorption and oxidation of CO on gold/titania model catalysts. Surface Science, 2007, 601, 3801-3804.	0.8	12
480	Adsorption of Supramolecular Building Blocks on Graphite: A Force Field and Density Functional Theory Study. ChemPhysChem, 2011, 12, 2242-2245.	1.0	12
481	Oxidation of an Organic Adlayer: A Bird's Eye View. Journal of the American Chemical Society, 2012, 134, 8817-8822.	6.6	12
482	Analysis of diamond surface channel field-effect transistors with AlN passivation layers. Journal of Applied Physics, 2013, 114, .	1.1	12
483	Ag on Pt(111): Changes in Electronic and CO Adsorption Properties upon PtAg/Pt(111) Monolayer Surface Alloy Formation. ChemPhysChem, 2015, 16, 2943-2952.	1.0	12
484	Photoâ€electrochemical Oxidation of Organic C1 Molecules over WO ₃ Films in Aqueous Electrolyte: Competition Between Water Oxidation and C1 Oxidation. ChemSusChem, 2015, 8, 3677-3687.	3.6	12
485	Study on the stability of Li2MnSiO4 cathode material in different electrolyte systems for Li-ion batteries. Electrochimica Acta, 2015, 176, 679-688.	2.6	12
486	Chemical and Electronic Changes of the CeO2 Support during CO Oxidation on Au/CeO2 Catalysts: Time-Resolved Operando XAS at the Ce LIII Edge. Catalysts, 2019, 9, 785.	1.6	12

#	Article	IF	CITATIONS
487	Interaction of Ultrathin Films of Ethylene Carbonate with Oxidized and Reduced Lithium Cobalt Oxide—A Model Study of the Cathode Electrolyte Interface in Liâ€ion Batteries. Advanced Materials Interfaces, 2019, 6, 1801650.	1.9	12
488	Dynamic changes of Au/ZnO catalysts during methanol synthesis: A model study by temporal analysis of products (TAP) and Zn LIII near Edge X-Ray absorption spectroscopy. Catalysis Today, 2019, 336, 193-202.	2.2	12
489	Surface Science and Electrochemical Model Studies on the Interaction of Graphite and Li ontaining Ionic Liquids. ChemSusChem, 2020, 13, 2589-2601.	3.6	12
490	Influence of water vapor on the performance of Au/ZnO catalysts in methanol synthesis from CO2 and H2: A high-pressure kinetic and TAP reactor study. Applied Catalysis B: Environmental, 2021, 297, 120416.	10.8	12
491	Adsorbate Covered Metal Surfaces and Reactions on Metal Surfaces. Springer Series in Surface Sciences, 1992, , 39-82.	0.3	12
492	Scanning Tunneling Microscopy: Metal Surfaces, Adsorption and Surface Reactions. , 1990, , 173-209.		12
493	Summary Abstract: Growth kinetics of an adsorbateâ€induced surface reconstruction. Journal of Vacuum Science and Technology A: Vacuum, Surfaces and Films, 1986, 4, 1411-1412.	0.9	11
494	Summary Abstract: Potassium on Ni(110) and Au(110): Adlayer ordering and/or surface reconstruction. Journal of Vacuum Science and Technology A: Vacuum, Surfaces and Films, 1987, 5, 794-796.	0.9	11
495	Electronically induced modifications of a-Si:H(P) films by scanning tunneling microscopy. Journal of Non-Crystalline Solids, 1991, 137-138, 1067-1070.	1.5	11
496	Luminescence properties and surface topography of porous silicon. Journal of Luminescence, 1993, 57, 211-215.	1.5	11
497	STM study of the Cl induced high temperature Si(111) (7 × 7) ↔ (1 × 1) phase transitions. Surface Science, 1994, 307-309, 216-222.	0.8	11
498	Electrodeposition of Ni on Cu(100): an in-situ STM study. Surface Science, 1997, 382, 107-115.	0.8	11
499	Surface Species and Product Distribution in the Electrooxidation of Small Organic Molecules. ECS Transactions, 2009, 25, 259-269.	0.3	11
500	Methanol, Formaldehyde, and Formic Acid Adsorption/Oxidation on a Carbon-Supported Pt Nanoparticle Fuel Cell Catalyst: A Comparative Quantitative DEMS Study. , 0, , 411-464.		11
501	Product gas evolution above planar microstructured model catalysts—A combined scanning mass spectrometry, Monte Carlo, and Computational Fluid Dynamics study. Journal of Chemical Physics, 2010, 133, 094504.	1.2	11
502	Electrochemistry at Ru(0001) in a flowing CO-saturated electrolyte—reactive and inert adlayer phases. Physical Chemistry Chemical Physics, 2011, 13, 6010.	1.3	11
503	Stabilization of Large Adsorbates by Rotational Entropy: A Timeâ€Resolved Variableâ€Temperature STM Study. ChemPhysChem, 2013, 14, 162-169.	1.0	11
504	A novel photoelectrochemical flow cell with online mass spectrometric detection: oxidation of formic acid on a nanocrystalline TiO ₂ electrode. Physical Chemistry Chemical Physics, 2014, 16, 25076-25080.	1.3	11

#	Article	IF	CITATIONS
505	Thermochemical Energy Storage through De/Hydrogenation of Organic Liquids: Reactions of Organic Liquids on Metal Hydrides. ACS Applied Materials & Interfaces, 2016, 8, 13993-14003.	4.0	11
506	Formation and removal of active oxygen species for the non-catalytic CO oxidation on Au/TiO 2 catalysts. Chinese Journal of Catalysis, 2016, 37, 1684-1693.	6.9	11
507	Interaction of CO with PtxAg1-x/Pt(111) surface alloys: More than dilution by Ag atoms. Surface Science, 2016, 650, 237-254.	0.8	11
508	Investigation on the Thermal Stability of Li ₂ MnSiO ₄ â€Based Cathodes for Liâ€ion Batteries: Effect of Electrolyte and State of Charge. Energy Technology, 2017, 5, 1561-1570.	1.8	11
509	Spectroscopic investigations on the origin of the improved performance of composites of nanoparticles/graphene sheets as anodes for lithium ion batteries. Carbon, 2018, 127, 47-56.	5.4	11
510	Adsorption of Ultrathin Ethylene Carbonate Films on Pristine and Lithiated Graphite and Their Interaction with Li. Langmuir, 2018, 34, 8451-8463.	1.6	11
511	Temperature-dependent insertion and adsorption of lithium on spinel Li ₄ Ti ₅ O ₁₂ (111) thin films – an angle-resolved XPS study. Physical Chemistry Chemical Physics, 2018, 20, 18319-18327.	1.3	11
512	Ionic Liquid Electrolytes for Metal-Air Batteries: Interactions between O ₂ , Zn ²⁺ and H ₂ O Impurities. Journal of the Electrochemical Society, 2020, 167, 070505.	1.3	11
513	Comment on â€~ã€~Layer-by-layer growth of Ag on Ag(111) induced by enhanced nucleation: A model study for surfactant-mediated growth''. Physical Review Letters, 1994, 73, 364-364.	2.9	10
514	Modification of the Si(111) 7 × 7 local electronic surface structure induced by silane adsorption. Chemical Physics Letters, 1995, 243, 445-449.	1.2	10
515	Atomistic modeling of the directed-assembly of bimetallic Pt-Ru nanoclusters on Ru(0001)-supported monolayer graphene. Journal of Chemical Physics, 2013, 138, 134703.	1.2	10
516	Temperature-induced structural and chemical changes of ultrathin ethylene carbonate films on Cu(111). Physical Chemistry Chemical Physics, 2014, 16, 11191-11195.	1.3	10
517	Electrochemical Behavior of Layered Vanadium Oxychloride in Rechargeable Lithium Ion Batteries. Journal of the Electrochemical Society, 2016, 163, A2326-A2332.	1.3	10
518	Oxygen Adsorption and Low-Temperature CO Oxidation on a Nanoporous Au Catalyst: Reaction Mechanism and Foreign Metal Effects. Topics in Catalysis, 2018, 61, 446-461.	1.3	10
519	The performance of structurally well-defined AgxPt1â^'x/Pt(111) surface alloys in the oxygen reduction reaction – An atomic-scale picture. Journal of Electroanalytical Chemistry, 2018, 819, 401-409.	1.9	10
520	Stability and ORR performance of a well-defined bimetallic Ag70Pt30/Pt(111) monolayer surface alloy electrode – Probing the de-alloying at an atomic scale. Electrochimica Acta, 2018, 259, 762-771.	2.6	10
521	Electrocatalytic Oxygen Reduction and Oxygen Evolution in Mgâ€Free and Mg–Containing Ionic Liquid 1â€Butylâ€1â€Methylpyrrolidinium Bis (Trifluoromethanesulfonyl) Imide. ChemElectroChem, 2018, 5, 2600-2611.	1.7	10
522	Electrochemical Formation and Characterization of Surface Blocking Layers on Gold and Platinum by Oxygen Reduction in Mg(ClO ₄) ₂ in DMSO. Journal of the Electrochemical Society, 2018, 165, A2037-A2046.	1.3	10

#	Article	IF	CITATIONS
523	Effect of Li + and Mg 2+ on the Electrochemical Decomposition of the Ionic Liquid 1â€Butylâ€1― methylpyrrolidinium bis(trifluoromethanesulfonyl)imide and Related Electrolytes. ChemElectroChem, 2019, 6, 3009-3019.	1.7	10
524	Pt nanocluster size effects in the hydrogen evolution reaction: approaching the theoretical maximum activity. Physical Chemistry Chemical Physics, 2020, 22, 19059-19068.	1.3	10
525	Influence of Complexing Additives on the Reversible Deposition/Dissolution of Magnesium in an Ionic Liquid. ChemElectroChem, 2021, 8, 390-402.	1.7	10
526	Dopant migration in silicon during implantation/annealing measured by scanning tunneling microscopy. Journal of Vacuum Science & Technology an Official Journal of the American Vacuum Society B, Microelectronics Processing and Phenomena, 1991, 9, 690.	1.6	9
527	Structures on Si(100)2 × 1at the Initial Stages of Homoepitaxy by SiH4Decomposition. Japanese Journal of Applied Physics, 1997, 36, 3804-3809.	0.8	9
528	Dissociative Adsorption of SiH ₂ Cl ₂ on Si(111)7×7. Zeitschrift Fur Physikalische Chemie, 1997, 198, 205-220.	1.4	9
529	Adsorption of disilane on Si(111)-(7×7) and initial stages of CVD growth. Surface Science, 1998, 416, 226-239.	0.8	9
530	Mechanisms of hole formation in metal-on-metal epitaxial systems: Rh/Ag(001). Surface Science, 2003, 524, L89-L95.	0.8	9
531	Controlled Surface Structure for In Situ ATR-FTIRS Studies Using Preferentially Shaped Pt Nanocrystals. Electrocatalysis, 2011, 2, 69-74.	1.5	9
532	The Adsorption of Oxygen and Coadsorption of CO and Oxygen on Structurally Wellâ€Đefined PdAg Surface Alloys. ChemPhysChem, 2012, 13, 3516-3525.	1.0	9
533	Adsorption and oxidation of formaldehyde on a polycrystalline Pt film electrode: An in situ IR spectroscopy search for adsorbed reaction intermediates. Beilstein Journal of Nanotechnology, 2014, 5, 747-759.	1.5	9
534	Potentialinduzierte OberflÃ e henrestrukturierung – die Bedeutung der strukturellen Charakterisierung in der Elektrokatalyse. Angewandte Chemie, 2014, 126, 13150-13154.	1.6	9
535	Novel, Highly Conductive Pt/TiO ₂ Thinâ€Film Model Catalyst Electrodes: The Role of Metal–Support Interactions. ChemElectroChem, 2016, 3, 1553-1563.	1.7	9
536	Influence of Step and Island Edges on Local Adsorption Properties: Hydrogen Adsorption on Pt Monolayer Island Modified Ru(0001) Electrodes. Electrocatalysis, 2017, 8, 530-539.	1.5	9
537	Structure, surface chemistry and electrochemical de-alloying of bimetallic PtxAg100-x nanoparticles: Quantifying the changes in the surface properties for adsorption and electrocatalytic transformation upon selective Ag removal. Journal of Electroanalytical Chemistry, 2017, 793, 164-173.	1.9	9
538	MnPO4 -Coated Li-NCM: MnPO4 -Coated Li(Ni0.4 Co0.2 Mn0.4)O2 for Lithium(-Ion) Batteries with Outstanding Cycling Stability and Enhanced Lithiation Kinetics (Adv. Energy Mater. 27/2018). Advanced Energy Materials, 2018, 8, 1870123.	10.2	9
539	Interaction between Li, Ultrathin Adsorbed Ionic Liquid Films, and CoO(111) Thin Films: A Model Study of the Solid Electrolyte Interphase Formation. Chemistry of Materials, 2019, 31, 5537-5549.	3.2	9
540	Atomic scale insights on the electronic and geometric effects in the electro-oxidation of CO on PtxRu1-x/Ru(0001) surface alloys. Electrochimica Acta, 2019, 306, 516-528.	2.6	9

#	Article	IF	CITATIONS
541	O2 reduction on a Au film electrode in an ionic liquid in the absence and presence of Mg2+ ions: Product formation and adlayer dynamics. Journal of Chemical Physics, 2019, 150, 041724.	1.2	9
542	Scanning tunneling microscopy investigations of corrosive processes on Si(111) surfaces. , 1991, , 189-200.		8
543	Scanning tunneling microscopy induced local deposition of Si or SiHx on Si(111)-(7×7). Journal of Vacuum Science & Technology an Official Journal of the American Vacuum Society B, Microelectronics Processing and Phenomena, 1995, 13, 1216.	1.6	8
544	Influence of SiH4deposition on the Si(111) 1×1→7×7 phase transition. Physical Review B, 1996, 54, R17284-R17287.	1.1	8
545	Nucleation and growth kinetics in semiconductor chemical vapor deposition. Physical Review B, 2001, 63, .	1.1	8
546	Direct Identification of Critical Clusters in Chemical Vapor Deposition. Physical Review Letters, 2006, 96, 116101.	2.9	8
547	α to γ phase transformation in electrodeposited Invar film by short pulse laser treatment. Materials Science & Engineering A: Structural Materials: Properties, Microstructure and Processing, 2007, 456, 64-71.	2.6	8
548	Model Studies on Solid Electrolyte Interphase Formation on Graphite Electrodes in Ethylene Carbonate and Dimethyl Carbonate II: Graphite Powder Electrodes. ChemElectroChem, 2020, 7, 4794-4809.	1.7	8
549	Investigation of the Anodeâ€Electrolyte Interface in a Magnesium Fullâ€Cell with Fluorinated Alkoxyborateâ€Based Electrolyte. Batteries and Supercaps, 2022, 5, .	2.4	8
550	Tetramer formation on Si(100)-(2 × 1) during CVD growth from SiH4. Surface Science, 1997, 377-379, 1001-1005.	0.8	7
551	Dissociative adsorption and site specificity in the initial stages of tetraethoxysilane (TEOS) interaction with Si(111)-(7×7). Surface Science, 1998, 400, 356-366.	0.8	7
552	Stability and chemisorption properties of ultrathin TiOx/Pt(111) films and Au/TiOx/Pt(111) model catalysts in reactive atmospheres. Physical Chemistry Chemical Physics, 2010, 12, 6864.	1.3	7
553	Nanostructured, mesoporous Au/TiO ₂ model catalysts – structure, stability and catalytic properties. Beilstein Journal of Nanotechnology, 2011, 2, 593-606.	1.5	7
554	The Role of Reactive Reaction Intermediates in Two-Step Heterogeneous Electrocatalytic Reactions: A Model Study. Fuel Cells, 2011, 11, 501-510.	1.5	7
555	Geometric and electronic structure of Au on Au/CeO ₂ catalysts during the CO oxidation: Deactivation by reaction induced particle growth. Journal of Physics: Conference Series, 2016, 712, 012044.	0.3	7
556	Selective Binding of Inhibitorâ€Assisted Surfaceâ€Imprinted Core/Shell Microbeads in Protein Mixtures. ChemistrySelect, 2018, 3, 4277-4282.	0.7	7
557	Morphologieâ€optimierte hochaktive und â€stabile Ru/TiO ₂ â€Katalysatoren für die selektive COâ€Methanisierung. Angewandte Chemie, 2019, 131, 10842-10847.	1.6	7
558	Ladungszustand von Auâ€Nanopartikeln wĤrend der Methanolsynthese aus CO ₂ /H ₂ an Au/ZnOâ€Katalysatoren: Einsichten aus Operando IRâ€Spektroskopie und Inâ€situ XPS―und XASâ€Messungen. Angewandte Chemie, 2019, 131, 10431-10436.	1.6	7

#	Article	IF	CITATIONS
559	How many electrons are transferred during the electrochemical O2 reduction in a Mg2+-free / Mg2+-containing ionic liquid?. Electrochimica Acta, 2019, 299, 372-377.	2.6	7
560	Adlayer growth vs spontaneous (near-) surface alloy formation: Zn growth on Au(111). Journal of Chemical Physics, 2020, 152, 124701.	1.2	7
561	Controlling the selectivity of high-surface-area Ru/TiO2 catalysts in CO2 reduction - modifying the reaction properties by Si doping of the support. Applied Catalysis B: Environmental, 2022, 317, 121748.	10.8	7
562	Structure of underpotential deposited metal adlayers observed by scanning tunnelling microscopy. Electrochimica Acta, 1991, 36, 1893-1894.	2.6	6
563	SÃ u rekorrosion und Korrosionsinhibition auf atomarem Maßstab. Materials and Corrosion - Werkstoffe Und Korrosion, 1998, 49, 169-174.	0.8	6
564	Scanning tunneling microscope mediated nanostructure fabrication from GeH4 on Si(111)-(7×7). Applied Physics Letters, 2003, 83, 3794-3796.	1.5	6
565	Mesoscopic Transport Effects in Electrocatalytic Reactions. ECS Transactions, 2010, 25, 91-102.	0.3	6
566	Growth of an oligopyridine adlayer on Ag(100) – A scanning tunnelling microscopy study. Physical Chemistry Chemical Physics, 2011, 13, 20724.	1.3	6
567	Spill-Over Effects on Bimetallic Pt/Ru(0001) Surfaces. Topics in Catalysis, 2013, 56, 1333-1344.	1.3	6
568	Interaction of Coadsorbed CO and Deuterium on a Bimetallic, Pt Monolayer Island Modified Ru(0001) Surface. Journal of Physical Chemistry C, 2014, 118, 28948-28958.	1.5	6
569	Influence of re-activation and ongoing CO oxidation reaction on the chemical and electronic properties of Au on a Au/CeO 2 catalyst: A XANES study at the Au L III edge. Journal of Electron Spectroscopy and Related Phenomena, 2017, 220, 86-90.	0.8	6
570	Lithium-Magnesium Hybrid Battery with Vanadium Oxychloride as Electrode Material. ChemistrySelect, 2017, 2, 7558-7564.	0.7	6
571	Electrooxidation of formic acid on a polycrystalline Au film electrode–A comparison with mass transport limited bulk CO oxidation and kinetically limited oxalic acid oxidation. Journal of Electroanalytical Chemistry, 2017, 800, 60-76.	1.9	6
572	Influence of Additives on the Reversible Oxygen Reduction Reaction/Oxygen Evolution Reaction in the Mg 2+ ontaining Ionic Liquid N â€Butyl―N â€Methylpyrrolidinium Bis(Trifluoromethanesulfonyl)imide. ChemSusChem, 2020, 13, 3919-3927.	3.6	6
573	Interaction of Mg with the ionic liquid 1-butyl-1-methylpyrrolidinium bis(trifluoromethylsulfonyl)imide—An experimental and computational model study of the electrode–electrolyte interface in post-lithium batteries. Journal of Vacuum Science and Technology A: Vacuum. Surfaces and Films. 2022. 40	0.9	6
574	Thermal decomposition of tetraethoxysilane (TEOS) on Si(111)-(7×7). Applied Physics A: Materials Science and Processing, 1998, 66, S1021-S1024.	1.1	5
575	Nanostructure formation by localized decomposition of Mo(CO)6 on Si(111)-(7×7) surfaces. Journal of Applied Physics, 2002, 91, 2853-2858.	1.1	5
576	Mass transport effects in CO adsorption and continuous CO electrooxidation over regular arrays of Pt nanostructures on planar glassy carbon supports. Journal of Electroanalytical Chemistry, 2011, 662. 157-168.	1.9	5

#	Article	IF	CITATIONS
577	Formic Acid Electrooxidation on a Au Electrode Studied by Potential Step and Fast Scan ATR-FTIR Spectroscopy. ECS Transactions, 2015, 66, 1-10.	0.3	5
578	Partial dissociation of water on Ru(0001) at low temperatures – Adsorption, structure formation and hydrogen passivation effects. Surface Science, 2018, 674, 32-39.	0.8	5
579	Calcium–Sulfur Batteries: Rechargeable Calcium–Sulfur Batteries Enabled by an Efficient Borateâ€Based Electrolyte (Small 39/2020). Small, 2020, 16, 2070216.	5.2	5
580	UHV preparation and electrochemical/-catalytic properties of well-defined Co– and Fe-containing unary and binary oxide model cathodes for the oxygen reduction and oxygen evolution reaction in Zn-air batteries. Journal of Electroanalytical Chemistry, 2021, 896, 115497.	1.9	5
581	Erratum to "Mesoscopic structural transformations of the Au(111) surface induced by alkali metal adsorption―[Surface Science Letters 302 (1994) L319–L324]. Surface Science, 1994, 312, L757.	0.8	4
582	In-Situ Stm Studies on the Electrodeposition of Ultrathin Nickel Films. Materials Research Society Symposia Proceedings, 1996, 451, 43.	0.1	4
583	The Nickel/Diamond(100)–(2 × 1)H Interface Studied with Electron Spectroscopy. Japanese Journal of Applied Physics, 1997, 36, 3635-3638.	0.8	4
584	Self-limited SiH2Cl2 gas source molecular beam epitaxy on Si(100). Surface Science, 2001, 491, 275-299.	0.8	4
585	Low-pressure microreactor system for kinetic studies on high surface area catalysts in the pressure gap. Review of Scientific Instruments, 2005, 76, 024102.	0.6	4
586	Multiple Wall-Jet Flow Cell Setup for Quantitative Parallel Evaluation of Carbon-Supported Electrocatalysts under Fuel Cell Relevant Conditions. Journal of the Electrochemical Society, 2008, 155, B908.	1.3	4
587	High Fidelity Selfâ€Recognition of Isomeric Oligopyridines in Binary 2D Selfâ€Assembly and Its Application for Separation. Chemistry - A European Journal, 2011, 17, 7831-7836.	1.7	4
588	Kinetically Limited CO Adsorption: Spillâ€Over as a Highly Effective Adsorption Pathway on Bimetallic Surfaces. ChemPhysChem, 2013, 14, 3801-3805.	1.0	4
589	Kinetic limitations in surface alloy formation: PtCu/Ru(0001). Surface Science, 2016, 643, 65-78.	0.8	4
590	Dynamics of the Interaction of Formic Acid with a Polycrystalline Pt Film Electrode: a Time-Resolved ATR-FTIR Spectroscopy Study at Low Potentials and Temperatures. Electrocatalysis, 2017, 8, 616-629.	1.5	4
591	Surface chemistry and electrochemistry of an ionic liquid and lithium on Li4Ti5O12(111)—A model study of the anode electrolyte interface. Journal of Chemical Physics, 2019, 151, 134704.	1.2	4
592	Ru(0001) surface electrochemistry in the presence of specifically adsorbing anions. Electrochimica Acta, 2021, 389, 138350.	2.6	4
593	Molecular and Dissociative Hydrogen Adsorption on Bimetallic PdAg/Pd(111) Surface Alloys: A Combined Experimental and Theoretical Study. Journal of Physical Chemistry C, 2022, 126, 3060-3077.	1.5	4
594	Chemisorption geometry of hydrogen on a Ni(111) surface. Surface Science, 1979, 89, 403.	0.8	3

#	Article	IF	CITATIONS
595	Local structures and processes on surfaces studied by scanning tunnelling microscopy. Journal of Physics Condensed Matter, 1991, 3, S117-S120.	0.7	3
596	PATTERN FORMATION IN METAL ON METAL EPITAXY. Fractals, 1994, 02, 183-189.	1.8	3
597	Electron spectroscopy study of the silverâ€diamond(100)â€H interface. Applied Physics Letters, 1996, 69, 4035-4037.	1.5	3
598	Mesoporous Silica and Titania by Glycol-Modified Precursors. Materials Research Society Symposia Proceedings, 2007, 1007, 1.	0.1	3
599	Atomistic modeling of Ru nanocluster formation on graphene/Ru(0001): Thermodynamically versus kinetically directed-assembly. Materials Research Society Symposia Proceedings, 2013, 1498, 249-254.	0.1	3
600	Vermeiden von Selbstvergiftung – ein Schlüsselaspekt für die hohe Aktivitävon Au/Mg(OH) ₂ â€Katalysatoren in der kontinuierlichen Niedertemperaturâ€COâ€Oxidation. Angewandte Chemie, 2017, 129, 9726-9731.	1.6	3
601	Challenges in bimetallic multilayer structure formation: Pt growth on Cu monolayers on Ru(0001). Physical Chemistry Chemical Physics, 2017, 19, 24100-24114.	1.3	3
602	Impact of Surface Chemistry and Doping Concentrations on Biofunctionalization of GaN/Ga‒In‒N Quantum Wells. Sensors, 2020, 20, 4179.	2.1	3
603	Intermixing and two-dimensional alloy formation in the Na/AAu(111) system. Surface Science Letters, 1993, 292, L769-L774.	0.1	2
604	Creation of electrically active nanoscale structures ina-Si films with a scanning tunneling microscope: Electronically induced changes in atomic bonding configurations. Physical Review B, 1994, 50, 17172-17179.	1.1	2
605	The role of antiphase domain boundaries in Si epitaxy by ultrahigh vacuum chemical vapor deposition from SiH 4 or SiH 2 Cl 2 on Si(100)-(2Ā—1). Applied Physics A: Materials Science and Processing, 1998, 66, S1025-S1029.	1.1	2
606	Mechanism of GeH4 dissociation on Si(111)-(7×7). Surface Science, 2003, 531, 265-271.	0.8	2
607	Electrocatalysis on the nm scale. Beilstein Journal of Nanotechnology, 2015, 6, 1008-1009.	1.5	2
608	Batteries: Performance Improvement of Magnesium Sulfur Batteries with Modified Nonâ€Nucleophilic Electrolytes (Adv. Energy Mater. 3/2015). Advanced Energy Materials, 2015, 5, .	10.2	2
609	Silanization of Sapphire Surfaces for Optical Sensing Applications. ACS Sensors, 2017, 2, 522-530.	4.0	2
610	Water and CO (co-)adsorption on pseudomorphic Pt films on Ru(0001) – a low-temperature scanning tunneling microscopy study. Physical Chemistry Chemical Physics, 2017, 19, 22434-22443.	1.3	2
611	Electronic effects on the water adsorption behaviour and structure formation on pseudomorphic Pt films on Ru(0001). Surface Science, 2018, 676, 30-38.	0.8	2

Revisiting the Electrochemical Lithiation Mechanism of Aluminum and the Role of Liâ \in rich Phases (Li 1+ x) Tj ETQqQ.0.0 rgBT [Overlock 1]

#	Article	IF	CITATIONS
613	Interaction between Li, Ultrathin Adsorbed Ethylene Carbonate Films, and CoO(111) Thin Films: A Model Study of the Solid Electrolyte Interphase Formation at CoO Anodes. Journal of Physical Chemistry C, 2020, 124, 21476-21490.	1.5	2
614	Interaction of bimetallic Zn/Au(111) surfaces with O2 or NO2 and formation of ZnOx/Au(111). Surface Science, 2021, 711, 121863.	0.8	2
615	Relaxation and Reconstruction on Ni(110) and Pd(110) Induced by Adsorbed Hydrogen. Springer Series in Surface Sciences, 1988, , 207-213.	0.3	2
616	Early Stages of Ni(110) Oxidation — An STM Study. Springer Series in Surface Sciences, 1988, , 261-266.	0.3	2
617	Resolving the structure of V ₃ O ₇ ·H ₂ O and Mo-substituted V ₃ O ₇ ·H ₂ O. Acta Crystallographica Section B: Structural Science, Crystal Engineering and Materials, 2022, 78, 637-642.	0.5	2
618	Tantalum deposition on and reaction with the hydrogen terminated diamond (100) surface studied by Auger electron and electron energy loss spectroscopy. Applied Physics Letters, 1996, 68, 2508-2510.	1.5	1
619	Dissociative Adsorption of SiH ₂ Cl ₂ on Si(111)7×7. Zeitschrift Fur Physikalische Chemie, 1997, 199, 123-123.	1.4	1
620	Irradiation-induced Ge multilayer growth from GeH4 on Si(111). Surface Science, 2000, 454-456, 811-817.	0.8	1
621	In-situ STM study of copper deposition on Cu(111) single-crystal electrode in sulfuric acid solution. , 2001, , .		1
622	Si x Ge 1-x ultrahigh-vacuum chemical vapor deposition on Si(111)(7×7) from GeH 4 /Si 2 H 6 mixtures. Applied Physics A: Materials Science and Processing, 2003, 76, 711-719.	1.1	1
623	Ag on Pt(111): Changes in Electronic and CO Adsorption Properties upon PtAg/Pt(111) Monolayer Surface Alloy Formation. ChemPhysChem, 2015, 16, 2907-2907.	1.0	1
624	The role of surface Pt on the coadsorption of hydrogen and CO on Pt monolayer film modified Ru(0001) surfaces. Surface Science, 2016, 652, 123-133.	0.8	1
625	Lithiumâ€lon Batteries: Introducing Highly Redoxâ€Active Atomic Centers into Insertionâ€Type Electrodes for Lithiumâ€lon Batteries (Adv. Energy Mater. 25/2020). Advanced Energy Materials, 2020, 10, 2070112.	10.2	1
626	Low-temperature nucleation and growth of Zn on Au(111) and thermal stability toward (surface) alloy formation. Journal of Chemical Physics, 2021, 155, 124704.	1.2	1
627	Competing Reconstruction Mechanisms in H/Ni(110). Springer Series in Surface Sciences, 1985, , 257-263.	0.3	1
628	Influence of regioisomerism in bis(terpyridine) based exciplexes with delayed fluorescence. Journal of Materials Chemistry C, 2022, 10, 7699-7706.	2.7	1
629	Summary Abstract: Reconstruction in a thin film: Epitaxial Pt on Pd(100). Journal of Vacuum Science and Technology A: Vacuum, Surfaces and Films, 1986, 4, 1524-1525.	0.9	0
630	Summary Abstract: Strong vertical intralayer distortions as a key structural feature in the (1×2)H reconstructed Ni(110) surface. Journal of Vacuum Science and Technology A: Vacuum, Surfaces and Films, 1987, 5, 793-794.	0.9	0

_	#	Article	IF	CITATIONS
	631	Improved design for an aluminum evaporator. Journal of Vacuum Science and Technology A: Vacuum, Surfaces and Films, 1997, 15, 2452-2454.	0.9	0
_	632	Rauscher, Braun, and Behm Reply:. Physical Review Letters, 2006, 97, .	2.9	0
	633	3rdGerman-Italian-Japanese Meeting of Electrochemists. Fuel Cells, 2009, 9, 191-191.	1.5	0
	634	Inside Cover: Imaging an Ionic Liquid Adlayer by Scanning Tunneling Microscopy at the Solid Vacuum Interface (ChemPhysChem 14/2011). ChemPhysChem, 2011, 12, 2502-2502.	1.0	0
	635	The durability of stainless steel bondings. Adhesion Adhesives and Sealants, 2016, 13, 26-31.	0.1	0
	636	Battery Technology: Nitrogen Rich Hierarchically Organized Porous Carbon/Sulfur Composite Cathode Electrode for High Performance Li/S Battery: A Mechanistic Investigation by Operando Spectroscopic Studies (Adv. Mater. Interfaces 19/2016). Advanced Materials Interfaces, 2016, 3, .	1.9	0
	637	Aktivierte Modifikation der TrÃgerâ€Metallâ€Wechselwirkungen als Schlüssel für hochaktive Ru/γâ€Al 2 O 3 â€Katalysatoren für die CO x ―Methanisierung. Angewandte Chemie, 2020, 132, 22951-22959.	1.6	0
	638	Lithium Metal Batteries: Reducing Capacity and Voltage Decay of Coâ€Free Li _{1.2} Ni _{0.2} Mn _{0.6} O ₂ as Positive Electrode Material for Lithium Batteries Employing an Ionic Liquidâ€Based Electrolyte (Adv. Energy Mater. 34/2020). Advanced Energy Materials, 2020, 10, 2070142.	10.2	0
	639	Unveiling the Intricate Intercalation Mechanism in Manganese Sesquioxide as Positive Electrode in Aqueous Znâ€Metal Battery (Adv. Energy Mater. 35/2021). Advanced Energy Materials, 2021, 11, 2170136.	10.2	0
	640	Topography Modification and Microscopic Motion on Metal Surfaces. Springer Series in Surface Sciences, 1988, , 92-101.	0.3	0
	641	Formation and Stability of a Metastable c(2×4)0 Structure on an Unreconstructed Ni(110) Surface. Springer Series in Surface Sciences, 1988, , 225-230.	0.3	0